The VirB4 Family of Proposed Traffic Nucleoside Triphosphatases: Common Motifs in Plasmid RP4 TrbE Are Essential for Conjugation and Phage Adsorption

Christian Rabel,[1] A. Marika Grahn,[2] Rudi Lurz,[1] and Erich Lanka[1]*

Max-Planck-Institut für Molekulare Genetik, Dahlem, D-14195 Berlin, Germany,[1] and Department of Biosciences and Institute of Biotechnology, Viikki Biocenter, FIN-00014 University of Helsinki, Finland[2]

Proteins of the VirB4 family are encoded by conjugative plasmids and by type IV secretion systems, which specify macromolecule export machineries related to conjugation systems. The central feature of VirB4 proteins is a nucleotide binding site. In this study, we asked whether members of the VirB4 protein family have similarities in their primary structures and whether these proteins hydrolyze nucleotides. A multiple-sequence alignment of 19 members of the VirB4 protein family revealed striking overall similarities. We defined four common motifs and one conserved domain. One member of this protein family, TrbE of plasmid RP4, was genetically characterized by site-directed mutagenesis. Most mutations in *trbE* resulted in complete loss of its activities, which eliminated pilus production, propagation of plasmid-specific phages, and DNA transfer ability in *Escherichia coli*. Biochemical studies of a soluble derivative of RP4 TrbE and of the full-length homologous protein R388 TrwK revealed that the purified forms of these members of the VirB4 protein family do not hydrolyze ATP or GTP and behave as monomers in solution.

The conjugative IncPα plasmid RP4 (60,099 bp) is of great interest in three respects. First, this broad-host-range plasmid is self-transmissible and involved in the active spread of antibiotic resistance genes among bacterial pathogens. Second, the RP4 transfer system is a potentially powerful tool for genetic manipulation of gram-positive and gram-negative bacteria and even eukaryotic cells, as conjugative DNA transfer to *Saccharomyces cerevisiae* (30) and Chinese hamster ovary cells (59) has been observed. Third, the RP4 transfer apparatus is related to type IV secretion systems, a class of macromolecule export machinery found in several bacteria pathogenic to mammals and plants (for a review, see reference 13). Hence, RP4 is a model system for studying bacterial conjugation and type IV secretion.

The transfer proteins of RP4 are grouped into two functional classes, defined as proteins involved in DNA processing (Dtr) and proteins involved in mating pair formation (Mpf) (for a review see reference 43). The Dtr system comprises the proteins that prepare the single strand of DNA to be transferred and the origin of transfer (*oriT*). The Mpf system, the pilus assembly machinery, is a proposed multiprotein complex that contains 12 plasmid-encoded proteins and spans both the inner and outer membranes (23). Conjugative pili, a prerequisite for DNA transfer, also serve as receptors for plasmid-specific phages. At present, functions for only three Mpf proteins are known: TrbC is the precursor of the pilin, a cyclic polypeptide (18), TraF is a maturation protease for TrbC (26), and *trbK* encodes the entry exclusion function (25).

Type IV secretion systems are macromolecule exporters for the delivery of effector molecules (13). The prototype of type IV secretion systems is the *Agrobacterium tumefaciens* Ti system, which mediates the export of oncogenic T-DNA to plant cells. Several pathogenic bacteria use type IV secretion systems; for example, *Bordetella pertussis* uses such a secretion system for liberation of the pertussis toxin (10), and *Helicobacter pylori* uses a secretion system for transfer of the CagA protein to gastric epithelial cells (for a review see reference 12). The gene organizations in various type IV secretion and Mpf systems of conjugative plasmids are very similar, and homologous proteins can be found throughout these systems. Although the exported substrates (DNA-protein intermediates, protein[s]) and the target cells (bacteria, plants, mammals) vary impressively, it has becomes more evident that these highly specialized systems utilize a common mechanism to assign their tasks.

A promising approach to unravel the function of type IV secretion systems is to study homologous proteins of various representatives. All defined type IV secretion machineries are composed of about 12 proteins, but at present only a few of these components have been characterized. The VirB2-like proteins, the subunits of the pili, are the only class of proteins whose role has been experimentally determined (for a recent review see reference 33). The VirB11-like proteins, which are cytoplasmic ATPases that form hexameric rings (35, 36, 45), are essential parts of the pilus assembly machinery. Although even a crystal structure is available (63), the real function of these proteins remains unknown. Until now the mechanism of none of the type IV secretion systems has been understood.

The VirB4 protein family is a class of homologous proteins named after the protein VirB4 encoded by *A. tumefaciens* Ti plasmids. High levels of similarity among *A. tumefaciens* pTiC58 VirB4, RP4 TrbE, R388 TrwK, F TraC, and *B. pertussis* PtlC have been reported (38, 51). At present, the best-studied members of this protein family are the VirB4 proteins encoded

* Corresponding author. Mailing address: Max-Planck-Institut für Molekulare Genetik, Abteilung Lehrach, Ihnestraße 73, Dahlem, D-14195 Berlin, Germany. Phone: 49 30 8413 1696. Fax: 49 30 8413 1130. E-mail: lanka@molgen.mpg.de.

by pTiA6 and pTiC58, which supposedly have identical functions. Ti VirB4 is a homodimeric or -multimeric inner membrane protein (14, 15, 52), which is essential for T-DNA export and which requires a type A nucleotide binding site for virulence (6, 19). An ATPase activity of pTiC58 VirB4 has been reported (52). However, the function(s) of none of the members of the VirB4 protein family is known.

The VirB4 homologue of RP4, the TrbE protein (94.4 kDa), is the largest essential component of the RP4 transfer machinery. A central feature of TrbE is a type A nucleotide binding site, also called Walker box A (38, 58). RP4 TrbE is a hydrophobic protein with a predicted transmembrane helix (TMH) at its N terminus. It has been proposed that TrbE is anchored in the cytoplasmic membrane via its TMH, thus stabilizing the postulated membrane-spanning Mpf complex together with the RP4 proteins TrbF, -I, and -L and TraF (23).

We asked whether members of the VirB4 protein family have common features and whether members of this protein family have coinciding biochemical properties. In this study we constructed a multiple-sequence alignment of the VirB4 protein family, in which we defined four common motifs and one conserved domain. Site-directed mutagenesis within the conserved motifs in RP4 TrbE revealed that Walker motifs A and B are essential for pilus production (Pil phenotype), propagation of plasmid-specific phages (donor-phage specificity; Dps phenotype), and DNA transfer ability (Tra phenotype) in *Escherichia coli*. We biochemically characterized two VirB4 homologous proteins, a soluble deletion derivative of RP4 TrbE that is active in vivo and the full-length TrwK protein of plasmid R388 (IncW). Neither of these proteins possessed ATPase or GTPase activity, and both proteins behaved as monomers in solution.

MATERIALS AND METHODS

Strains, plasmids, and phages. *E. coli* K-12 strain SCS1 (a DH1 derivative [29]) was used as the standard strain for molecular cloning and protein overproduction. In special cases BL21 and BL21 Star(DE3)(pLysS) (Invitrogen) were used. *E. coli* K-12 strain HB101 (8) and the nalidixic acid-resistant derivative HB101 Nx^r were used for conjugation experiments. JE2571 (*leu thr fla pil str*) (9) was used for phage sensitivity assays and electron microscopy. Cells were grown in YT medium (40) buffered with 25 mM 3-(*N*-morpholino)propanesulfonic acid (sodium salt; pH 8.0) and supplemented with 0.1% glucose and 25 μg of thiamine hydrochloride per ml. For YT agar plates, 1.5% agar-agar was added to YT medium. When appropriate, antibiotics were added at the following concentrations: ampicillin (sodium salt), 100 μg/ml; chloramphenicol, 10 μg/ml; and nalidixic acid (sodium salt), 30 μg/ml. *A. tumefaciens* Agro 6000 (obtained from Barbara Hohn) harboring pTiA6 was grown on YT agar plates for 2 days at room temperature. Phages PRD1, PRR1, and Pf3 were propagated as described previously (55). The plasmids and phages used are shown in Table 1.

Buffers. Buffer A contained 20 mM Tris-HCl (pH 7.6), 150 mM NaCl, 1 mM dithiothreitol (DTT), 0.1 mM EDTA, and 10% (wt/vol) glycerol. Buffer B contained 20 mM Tris-HCl (pH 7.6) and 150 mM NaCl. Buffer C contained 20 mM potassium phosphate (pH 6.8), 50 mM KCl, 1 mM DTT, and 10% (wt/vol) glycerol. Buffer D contained 20 mM imidazole (pH 7.6), 20 mM Tris-HCl (pH 7.6), 1 M NaCl, and 10% (wt/vol) glycerol. Buffer E contained 20 mM Tris-HCl (pH 7.6), 200 mM NaCl, 2 mM DTT, 0.1% (wt/vol) Brij 58, 0.1 mM EDTA, and 10% (wt/vol) glycerol. Buffer F contained 20 mM Tris-HCl (pH 7.6), 150 mM NaCl, and 1 mM DTT. HBS-EP buffer (BIAcore) contained 0.01 M HEPES (pH 7.4), 0.15 M NaCl, 3 mM EDTA, and 0.005% (wt/vol) polysorbate 20.

DNA techniques. Standard molecular cloning techniques were performed as described by Sambrook et al. (46). Unless noted otherwise, *Pfu* DNA polymerase (Stratagene) was used for PCR. The nucleotide sequences of cloned and mutated genes and of the in-frame deletion of *trbE* were confirmed. Overexpressed genes were placed under control of the *tac* promoter and the T7 gene *10* Shine-Dalgarno sequence (47).

Molecular cloning of RP4 *trbE* and construction of *trbE* mutants. Plasmid pCR21 was constructed by inserting the 2,670-bp *Hin*dIII-*Eco*RI fragment from pKW21Δ1 into pMS119HEΔ(*Hin*dIII-*Eco*RI). *trbE* mutants were constructed by PCR (Table 2) by using pCR21 as the template.

The *trbE* in-frame deletion was constructed by using an ExSite PCR-based site-directed mutagenesis kit (Stratagene) and pCR2001 as the template. pCR2001 was constructed by inserting the 4,369-bp *Nde*I-*Rsr*II fragment of pML123 in antitranscriptive orientation into pCR2000. Following mutagenesis, pCR2001Δ*trbE* was digested with *Nde*I and *Rsr*II, and the 1,838-bp fragment was inserted into pML123Δ(*Nde*I-*Rsr*II), resulting in pML123Δ*trbE*. pMS123Δ*trbE* was constructed by inserting the 2,629-bp *Aat*II-*Fse*I fragment of pML123Δ*trbE* into pMS123Δ(*Aat*II-*Fse*I). pDB126Δ*trbE* was constructed by inserting the 3,478-bp *Nde*I-*Bss*SI fragment of pML123Δ*trbE* into pDB126Δ(*Nde*I-*Bss*SI).

Amino acids were substituted by using the PCR-based method described by Weiner et al. (60). The alleles are designated X000Z below, where X is the wild-type residue, 000 is the residue number in the full-length protein, and Z is the newly introduced residue. The N-terminal deletion mutants TrbEΔ1, -2, and -4 to -6 were constructed by using forward primers (Table 2) and reverse primer GAGCGCCGGCGACAGCGGCGG (RP4 coordinates 21,948 to 21,928). Amplified DNA was digested with *Nde*I and *Dra*III and inserted into plasmids pCR21Δ(*Nde*I-*Dra*III) and pCR21HNΔ(*Nde*I-*Dra*III). Mutant TrbEΔ3 was constructed by using the ExSite PCR-based site-directed mutagenesis kit (Stratagene). The C-terminal deletions TrbEΔ7 to -11 were constructed by using forward primer CTCGACAAGTTCCGCAAGAAGTG (RP4 coordinates 21,505 to 21,527) and the reverse primers that generated a premature stop codon (Table 2). The amplified fragments were digested with *Dra*III and *Eco*RI and inserted into pCR21Δ(*Dra*III-*Eco*RI).

Molecular cloning of R388 *trwK* and pTiA6 *virB4*. Both R388 *trwK* and pTiA6 *virB4* were cloned by using PCR and the primers listed in Table 1. For *trwK*, pSU4054 was used as the template. The 2,474-bp fragment was digested with *Nde*I and *Eco*RI and inserted into pCR21Δ(*Nde*I-*Eco*RI), resulting in pCR38. *virB4*, including its original ribosome binding site, was amplified by using an aqueous extract of *A. tumefaciens* Agro 6000 cells as the template. The amplified DNA was digested with *Xma*I and *Sac*I, and the 2,530-bp fragment was inserted into pMS119HEΔ(*Xma*I-*Sac*I), resulting in plasmid pCRA6. Plasmid pCR6 was constructed by using pCRA6 as the template and inserting the 2,436-bp *Nde*I-*Sac*I fragment into pCR21Δ(*Nde*I-*Sac*I).

In vivo complementation assays. The strains used for the in vivo complementation assays are shown in Table 3. Standard phage plaque assays for studying the Dps phenotype were performed as described previously (27). ^{14}C-labeled PRD1 phage adsorption assays were performed as described previously (34). Pili were visualized by electron microscopy as described previously (9, 26). Mating for studying the Tra phenotype was carried out as described previously (2).

Sequence alignment of members of the VirB4 protein family. A BLAST search (1) with RP4 TrbE as the query was performed at the National Center for Biotechnology Information (http://www.ncbi.nlm.nih.gov/blast/). Based on the search results, 18 representative proteins with significant similarity to RP4 TrbE were chosen. The sequences were aligned by using the Clustal W software (57) with the BLOSUM series as the protein weight matrix. The alignment was shaded by using the freeware BOXSHADE 3.21 (K. Hofmann and M. D. Baron, http://www.ch.embnet.org/software/BOX_form.html).

Protein production. All protein production operations were carried out at 4°C unless noted otherwise. SCS1 cells harboring the expression plasmid (two 1.2-liter cultures in 5-liter flasks) were grown with aeration at 37°C to an A_{600} of 0.6. Isopropyl-β-thiogalactopyranoside (IPTG) was added to a final concentration of 10 μM to strain SCS1(pCR21HNΔ2) cultures and to a final concentration of 1 mM to strain SCS1(pCR38) and BL21(pCR6, pACYC-RIL) cultures. Incubation was continued for 5 h. Cells were harvested by centrifugation at 4,000 × g for 7 min and resuspended in a spermidine solution (20 mM spermidine · 3HCl, 200 mM NaCl, 2 mM EDTA; final volume, 50 ml). Cells were frozen in liquid nitrogen and stored at −80°C. After purification, proteins were stored at −20°C.

Purification of RP4 TrbEHNΔ2. Cells (13.5 g, wet weight) were thawed and lysed in the presence of a solution containing 50 mM Tris-HCl (pH 7.6), 1 M NaCl, 5% sucrose, 0.3 mg of lysozyme per ml, 0.13% Brij 58, 0.05 mM EDTA, and 0.05 mM EGTA. After centrifugation at 100,000 × g for 30 min, supernatant I was collected. The pellet was resuspended in 1 M NaCl–100 mM Tris-HCl (pH 7.6)–10% sucrose at 0°C by using a glass homogenizer and centrifuged at 100,000 × g for 30 min. Supernatant II was collected, pooled with supernatant I, and dialyzed against buffer B. The resulting sample (fraction I, 309 ml) (Table 4 and Fig. 1A, lane d) was loaded onto an Ni-nitrilotriacetic acid SF column equilibrated with buffer B. The column was washed with buffer D, and the proteins were eluted with buffer D containing 250 mM imidazole (pH 7.6). The peak fractions were pooled, dialyzed against buffer A (fraction II, 65 ml) (Table 4 and

TABLE 1. Plasmids and phages

Plasmid or phage	Description[a]	Relevant genotype	Selective marker[b]	Replicon	Source or reference
pACYC-RIL		*argU ileY leuW*	Cm	p15A	Stratagene
pCR6	pCR21Δ[*Nde*I-*Sac*I]Ω[pTiA6 *Nde*I-*Sac*I 152,657–155,086][c]	*virB4*⁺	Ap	pMB1	This study
pCR21	pMS119HEΔ[*Hin*dIII-*Eco*R1]Ω[pKW21Δ1 *Hin*dIII-*Eco*RI 2,670-bp fragment, RP4 20,545–23,127], P*tac*/*lacI*q	*trbE*⁺	Ap	pMB1	This study
pCR21HN	pCR21Δ[*Xba*I-*Nde*I]Ω[*Xba*I-*Nde*I adaptor][d]	*his₆-trbE*⁺	Ap	pMB1	This study
pCR21Δ1[e]	pCR21Δ[RP4 20,548–20,607]	*trbEΔ1*⁺	Ap	pMB1	This study
pCR21Δ2[e]	pCR21Δ[RP4 20,548–20,625]	*trbEΔ2*⁺	Ap	pMB1	This study
pCR21HNΔ2[e]	pCR21HNΔ[RP4 20,548–20,625]	*his₆-trbEΔ2*⁺	Ap	pMB1	This study
pCR21Δ3[e]	pCR21Δ[RP4 20,620–20,661]	*trbEΔ3*⁺	Ap	pMB1	This study
pCR21Δ4[e]	pCR21Δ[RP4 20,548–20,706]	*trbEΔ4*⁺	Ap	pMB1	This study
pCR21HNΔ5[e]	pCR21HNΔ[RP4 20,548–21,039]	*his₆-trbEΔ5*⁺	Ap	pMB1	This study
pCR21HNΔ6[e]	pCR21HNΔ[RP4 20,548–21,519]	*his₆-trbEΔ6*⁺	Ap	pMB1	This study
pCR21Δ7[e]	pCR21Δ[RP4 23,086–23,127]	*trbEΔ7*⁺	Ap	pMB1	This study
pCR21Δ8[e]	pCR21Δ[RP4 23,068–23,127]	*trbEΔ8*⁺	Ap	pMB1	This study
pCR21Δ9[e]	pCR21Δ[RP4 23,053–23,127]	*trbEΔ9*⁺	Ap	pMB1	This study
pCR21Δ10[e]	pCR21Δ[RP4 23,014–23,127]	*trbEΔ10*⁺	Ap	pMB1	This study
pCR21Δ11[e]	pCR21Δ[RP4 22,945–23,127]	*trbEΔ11*⁺	Ap	pMB1	This study
pCR38	pCR21Δ[*Nde*I-*Eco*RI]Ω[R388 1,025–3,496][f]	*trwK*⁺	Ap	pMB1	This study
pCR2000	pMS470Δ8Δ[*Eco*RI-*Hin*dIII]Ω[adaptor *Eco*RI-*Rsr*II-*Sac*I-*Age*I-*Kpn*I-*Nde*I-*Hin*dIII], cloning vector, P*tac*/*lacI*qg		Ap	pMB1	This study
pCR2001	pCR2000Δ[*Rsr*II-*Nde*I]Ω[pML123 *Rsr*II-*Nde*I 4,370-bp RP4 24,301–19,932]	(*trbD* to *trbF*)⁺, antitranscriptive orientation	Ap	pMB1	This study
pCR2001Δ*trbE*	pCR2001Δ[RP4 23,088–20,557]	*trbE*⁰	Ap	pMB1	This study
pCRA6	pMS119HEΔ[*Xma*I-*Sac*I]Ω[pTiA6 *Xma*I-*Sac*I 152,568–155,086][h]	Original RBS, *virB4*⁺	Ap	pMB1	This study
pCR21X000Z[e]	Amino acid substitutions	*trbE*⁺, mutation indicated	Ap	pMB1	This study
pDB126	pML123Ω[*Bam*HI; RP4 *Bfa*I 45,893–53,462 bp]	(*trbB* to *trbM*)⁺ (*traF* to *traM*)⁺ *oriT*⁺	Cm	ColD	2
pDB126Δ*trbE*	pDB126Δ[RP4 20,557–23,088 bp]	(*trbB* to *trbD*, *trbF* to *trbM*)⁺ (*traF* to *traM*)⁺ *oriT*⁺ *trbE*⁰	Cm	ColD	This study
pGZ119EH, HE	Cloning vector, P*tac*/*lacI*q		Cm	ColD	37
pKW21Δ1	pMS67HEΩ[mKW21*trbF*:*Bgl*II, 2.6 kb]	*trbE*⁺	Ap	RSF1010	27
pML123	pGZ119EHΔ[*Eco*RI-*Bam*HI]Ω[*Eco*RI-*Xmn*I adaptor, RP4 *Xmn*I-*Not*I, 18,841–30,042 bp]	(*trbB* to *trbM*)⁺	Cm	ColD	39
pML123Δ*trbE*	pMS123Δ[RP4 20,557–23,088 bp]	(*trbB* to *trbD*, *trbF* to *trbM*)⁺ *trbE*⁰	Cm	ColD	This study
pMS119EH, HE	Cloning vector, P*tac*/*lacI*q		Ap	pMB1	56
pMS123	pML123Δ[*Bam*HI-*Hin*dIII]Ω[*Bam*HI-*Xba*I adaptor, pWP471 *Xba*I-*Hin*dIII; RP4 18,841–30,042 and 45,909–46,577 bp][i]	(*trbB* to *trbM*)⁺ (*traF*)⁺	Cm	ColD	This study
pMS123Δ*trbE*	pMS123Δ[RP4 20,557–23,088 bp]	(*trbB* to *trbD*, *trbF* to *trbM*)⁺ (*traF*)⁺ *trbE*⁰	Cm	ColD	This study
pMS470Δ8	pMS119EHΔ[*Xba*I-*Pst*I]Ω[pT7-7 *Xba*I-*Nde*I, 40-bp fragment, R751 *traC Ava*I-*Sph*I, 1.4 kb], cloning vector, P*tac*/*lacI*q	*traC*⁺	Ap	pMB1	3
pSU4054	Plasmid encoding R388 TraW	*trwK*⁺ (among others)	Ap	pMB8	7
M13 mp18	Filamentous ssDNA phage; IncF specific				62
Pf3	Filamentous ssDNA phage; IncP specific				55
PRD1	Lipid-containing dsDNA phage; IncP, IncW, IncN specific				4
PRR1	RNA phage; IncP specific				42

[a] The accession numbers of the RP4, R388, and pTiA6 sequences are L27758, X81123, and AF242881, respectively.

[b] Ap, ampicillin; Cm, chloramphenicol.

[c] The following primers were used (nucleotides derived from the original sequence are in italics, and restriction sites are underlined): ATATATAT<u>CAT</u>*ATGC*TCGGCGCGAGTGGAACG and TATATA<u>GAGCTC</u>*GAAAGCTGCAGGTCAAAACCGTTGC*.

[d] The adaptor was as follows: CTAGAAATAATTTTGTTTAACTTTAAGAAGGAGATATACACATGCACCATCACCATCACCA
TTTATTAAAACAAATTGAAATTCTTCCTCTATATGTGTACGTGGTAGTGGTAGTGGTAT

[e] For the mutagenesis strategy used, see Materials and Methods.

[f] The following primers were used: ATATATAT<u>CAT</u>*ATGGGGGG*CAATTGAATCCCGCAAGCTCC and ATATATAT<u>GAATTC</u>*TCATACGTCGCTCCTTTCGGCTTTCACACGG*.

[g] The adaptor was as follows: AATTCCGGTCCGGAGCTCACCGGTGGTACCCATATGA
GGCCAGGCCTCGAGTGGCCACCATGGGTATACTTCGA

[h] The following primers were used: TATATA<u>CCCGGG</u>*GGAAGAAGCATTGATAGTGCAGTTTGGGG* and TATATA<u>GAGCTC</u>*GAAAGCTGCAGGTCAAAACCGTTGC*.

[i] The adaptor was as follows: GATCCGCGGT
GCGCCAGATC

TABLE 2. RP4 TrbE mutant phenotypes

trbE allele	Mutation	Transfer frequency[a]	Dps[b]				Pilus formation[c]	Oligonucleotide(s) used[d]
			PRD1	PRR1	Pf3	PRD1 adsorption (%)[e]		
pDB126[f]		1.6×10^{-1}	+	+	+	50.4	+	
trbE		4.1×10^{-2}	+	+	+	38.8	+	
ΔtrbE	In-frame deletion	$<1 \times 10^{-7}$	−	−	−	0.7	−	TGCTTGGATCATCGGTATTGCTTC (20,556-20,533), CTGGAGGCAGCATGAGTTTTG (23,089–23,103)
trbEHN	N-terminal His₆ tag	3.6×10^{-2}	+	+	+	40	+	
trbEH484A	Near motif A	2.7×10^{-2}	+	+	+	12	+	CGTTCCGGCTGAACCTG**GC**CGTGCGCGACCTCGG (21,976–22,010)
trbEG495A	Motif A	5.8×10^{-3}	+	+	+	14	+	CCACACCTTTATGTTCG**C**GCCGACCGGCGCAGG (22,011–22,043)
trbEG500A	Motif A	$<1 \times 10^{-7}$	−	−	−	0.7	−	CGGGCCGACCGGCGCAG**C**TAAATCGACGCACC (22,026–22,057)
trbEK501A	Motif A	1.7×10^{-4}	−	(+)	(+)	1.6	−	CCGACCGGCGCAGGT**GC**ATCGACGCACCTGGCG (22,030–22,062)
trbEK501E	Motif A	$<1 \times 10^{-7}$	−	−	−	0.6	−	CCGACCGGCGCAGGT**GC**ATCGACGCACCTGGCG (22,030–22,062)
trbES502A	Motif A	$<1 \times 10^{-7}$	−	−	−	0.9	−	CGACCGGCGCAGGTAAA**G**CGACGCACCTGGCGATCC (22,031–22,062)
trbED642A	Motif C	$<1 \times 10^{-7}$	−	−	−	0.8	−	GGGCCATCTGCTCG**C**CGCCGAAGAGGACGGC (22,455–22,485)
trbED642N	Motif C	$<1 \times 10^{-7}$	−	−	−	0.8	−	GGGCCATCTGCTC**AA**CGCCGAAGAGGACGGC (22,455–22,485)
trbED642N/ D694N	Motifs C and B	$<1 \times 10^{-7}$	−	−	−	1.0	−	GGGCCATCTGCTC**A**ACGCCGAAGAGGACGGC (22,455–22,485), GCCGTCATCATCCTG**A**ACGAAGCCTGGTTGATGC (22,609–22,642)
trbED646A	Motif C	2.9×10^{-2}	+/−	+	+	7.8	−	GCTCGACGCCGAAGAGG**C**CGGCTTGGCGCTGTCCG (22,464–22,498)
trbED694A	Motif B	$<1 \times 10^{-7}$	−	−	−	0.6	−	GCCGTCATCATCCTGGC**C**GAAGCCTGGTTGATGC (22,609–22,642)
trbED694N	Motif B	$<1 \times 10^{-7}$	−	−	−	0.8	−	GCCGTCATCATCCTG**A**ACGAAGCCTGGTTGATGC (22,609–22,642)
trbEE695A	Motif B	$<1 \times 10^{-7}$	−	−	−	0.7	−	CCGTCATCATCCTGGACG**C**AGCTGGTTGATGCTCG (22,610–22,645)
trbEE695Q	Motif B	$<1 \times 10^{-7}$	−	−	−	0.7	−	CCGTCATCATCCTGGAC**C**CAAGCTGGTTGATGCTCG (22,610–22,645)
trbER717A	Motif D	3.9×10^{-6}	−	(+)	(+)	1.1	+	GGCTCAAGGTGCTG**GC**TAAGGCCAACTGCC (22,679–22,708)
trbEQ728A	Motif D	5.2×10^{-3}	+	+	+	21.9[g]	+	GCTGATGGCAACG**GC**GAGCCTGTCCGACG (22,713–22,741)
trbEY766A	Near motif D	4.2×10^{-2}	+	+	+	38.7[g]	+	GGACACGGCGGCCCTG**GC**CGCCGCATGGGCC (22,824–22,855)
trbEY766F	Near motif D	6×10^{-2}	+	+	+	46.9[g]	+	GGACACGGCGGCCCTG**T**TCCGCCGCATGGGCC (22,824–22,855)
trbEΔ1	N terminus	4.5×10^{-4}	−	−	−	0.7	−	ATATATATCAT*ATGGCCCGCATCCGCGCGGTCGAT*G (20,608–20,629)
trbEΔ2	N terminus	1.3×10^{-2}	+	+	+	35.8	+	GGGAATTTCAT*ATGGATGCCGAACTGAAACTGAAAAAGCATC* (20,626–20,653)
trbEHNΔ2	N terminus	1.8×10^{-2}	+	+	+	32	+	GGGAATTTCAT*ATGGATGCCGAACTGAAACTGAAAAAGCATC* (20,626–20,653)
trbEΔ3	N terminus	$<1 \times 10^{-7}$	−	−	−	0.8	−	GCGGATGCGGGCAAAGAGGATGAAC (20,619–20,595), GACGCCGGCCTGGCCGATCTGC (20,662–20,683)
trbEΔ4	N terminus	$<1 \times 10^{-7}$	−	−	−	0.7	−	GGGAATTCAT*ATGGACGGCGTAATCGTGGGCAAGAAC* (20,707–20,730)
trbEHNΔ5	N terminus	$<1 \times 10^{-7}$	ND[h]	ND	ND	ND	ND	TATATATCAT*ATGTTCGTCGAGCTGATGTTTGACGACG* (21,043–21,070)
trbEHNΔ6	N terminus	$<1 \times 10^{-7}$	ND	ND	ND	ND	ND	ATATATATCAT*ATGAAGAAGTGGCGGCAGAAGATTCGC* (21,520–21,543)
trbEΔ7	C terminus	4×10^{-2}	+	+	+	44	+	CCCCCCGGAATTC*TCATTCATCAAGGGCGAGGCCCCGGCC* (23,085–23,062)
trbEΔ8	C terminus	9.3×10^{-2}	+	+	+	38	+	CCCCCCGGAATTC*TCACCGGCCACGCAGCCATTCATCCACCC* (23,067–23,042)
trbEΔ9	C terminus	$<1 \times 10^{-7}$	−	−	−	0.8	−	CCCCCCGGAATTC*TCATTCATCCACCCACTGGTCGCCG* (23,052–23,031)
trbEΔ10	C terminus	$<1 \times 10^{-7}$	−	−	−	0.9	−	CCCCCCGGAATTC*TCACTTGATGATGGCGACGGATTCCTTGTCGG* (23,013–22,985)
trbEΔ11	C terminus	$<1 \times 10^{-7}$	−	−	−	0.9	−	CCCCCCGGAATTC*TCAGTCGTAGAGACGGCGGCCGTTTTC* (22,944–22,921)

[a] Number of transconjugants per donor cell. The frequencies are average values for three independent experiments.
[b] +, Dps positive; +/−, Dps reduced; (+), weak Dps; −, Dps negative.
[c] +, pili found; −, no pili found.
[d] For amino acid substitutions, only the transcriptive strand primer is shown. Nucleotides derived from the original sequence are in italics; mutagenized nucleotides are in boldface type. The RP4 nucleotide coordinates are given in parentheses according to previously published sequence data (accession no. L27758).
[e] Relative amount of label associated with the cell pellet. ^{14}C-labeled PRD1 was adsorbed to the cells, incubated at 24°C for 15 min, and washed twice with YT medium. Radioactivity was determined in the cell and in the supernatant fractions.
[f] The trbE gene was encoded by plasmid pDB126.
[g] Phages were loosely bound to the cells.
[h] ND, not determined.

Fig. 1A, lane e), and loaded onto a heparin Sepharose CL-6B column equilibrated with the same buffer. The column was washed with equilibration buffer, and then proteins were eluted with a linear gradient of buffer A containing 150 to 600 mM NaCl. TrbEHNΔ2 eluted at 250 mM NaCl. The peak fractions were pooled and dialyzed against buffer F (fraction III, 49 ml) (Table 4 and Fig. 1A, lane f). Solid ammonium sulfate was added to a final concentration of 1 M, and the solution was loaded onto a phenyl Sepharose 6 Fast Flow column equilibrated with buffer F containing 1 M $(NH_4)_2SO_4$. The column was washed first with the equilibration buffer, then with buffer F, and finally with buffer F containing 40% (vol/vol) ethylene glycol. The proteins were eluted with a linear gradient of buffer F containing 40 to 70% (vol/vol) ethylene glycol. TrbEHNΔ2 eluted at 53% ethylene glycol. The peak fractions were combined, concentrated by dialysis against 20% polyethylene glycol 20,000 in buffer A, and then dialyzed against 50% glycerol in buffer A (fraction IV, 16.4 ml) (Table 4 and Fig. 1A, lane g).

Purification of R388 TrwK. Cells (14.7 g, wet weight) were thawed and lysed in the presence of a solution containing 50 mM Tris-HCl (pH 7.6), 100 mM NaCl, 5% sucrose, 0.3 mg of lysozyme per ml, 0.13% Brij 58, 0.05 mM EDTA, and 0.05 mM EGTA. After centrifugation at $100,000 \times g$ for 30 min, the supernatant was adjusted with solid ammonium sulfate to a saturation of 50% (16), stirred for 30 min at 0°C, and centrifuged at $100,000 \times g$ for 30 min. The precipitate was resuspended in buffer A containing 50 mM NaCl (fraction I, 56 ml) (Table 4 and Fig. 1B, lane d) at 0°C and applied to a heparin Sepharose CL-6B column equilibrated with buffer A containing 50 mM NaCl. The column

TABLE 3. Strains used for *trbE* complementation

Strain	Relevant genotype	Phenotype[a]		
		Pil	Dps	Tra
JE2571(pMS123)	$(trbB$ to $trbM)^+$ $(traF)^+$	+	+	NA
JE2571(pMS123$\Delta trbE$)	$(trbB$ to $trbD$, $trbF$ to $trbM)^+$ $(traF)^+$ $trbE^0$	−	−	NA
JE2571(pMS123$\Delta trbE$, pCR21)[b]	$(trbB$ to $trbD$, $trbF$ to $trbM)^+$ $(traF)^+$ $trbE^{+b}$	?	?	NA
HB101(pDB126)	$(trbB$ to $trbM)^+$ $(traF$ to $traM)^+$ $oriT^+$	NA	NA	+
HB101(pDB126$\Delta trbE$)	$(trbB$ to $trbD$, $trbF$ to $trbM)^+$ $(traF$ to $traM)^+$ $oriT^+$ $trbE^0$	NA	NA	−
HB101(pDB126$\Delta trbE$, pCR21)[b]	$(trbB$ to $trbD$, $trbF$ to $trbM)^+$ $(traF$ to $traM)^+$ $oriT^+$ $trbE^{+b}$	NA	NA	?

[a] +, positive; −, negative; ?, depends on the mutation; NA, not applicable. For experimental details see Materials and Methods.
[b] Plasmid pCR21 carried either the wild-type *trbE* allele (pCR21) or a *trbE* mutation (pCR21X000Z or pCR21Δ1–11) (Table 2).

was washed with the same buffer, and the proteins were eluted with a linear gradient of buffer A containing 50 to 600 mM NaCl. TrwK eluted at 140 mM NaCl. The peak fractions were pooled (fraction II, 67 ml) (Table 4 and Fig. 1B, lane e) and loaded onto a hydroxyapatite Bio-Gel HT column equilibrated with buffer C. The column was washed with buffer C, and the proteins were eluted with a linear gradient of buffer C containing 20 to 400 mM potassium phosphate (pH 6.8). TrwK eluted at 180 mM potassium phosphate. The peak fractions were pooled and dialyzed against buffer A containing 50 mM NaCl (fraction III, 103 ml) (Table 4 and Fig. 1B, lane f). Fraction III was loaded onto a DEAE Sephacel column equilibrated with buffer A containing 50 mM NaCl and washed with the same buffer. The proteins were eluted with a linear gradient of buffer A containing 50 to 600 mM NaCl. TrwK eluted at 300 mM NaCl. The peak fractions were combined, concentrated by dialysis against 20% polyethylene glycol 20,000 in buffer A, and then dialyzed against buffer A containing 50% glycerol and 100 mM NaCl (fraction IV, 12.7 ml) (Fig. 1B, lane g).

NTPase assays. Nucleoside triphosphate (NTP) hydrolysis experiments were performed with 1.5 μM purified protein at 30°C for 30 min in 20-μl (final volume) mixtures containing 20 mM Tris-HCl (pH 7.6), 100 mM NaCl, 5 mM MgCl$_2$, 0.05 mg of bovine serum albumin (BSA) per ml, 1 mM DTT, 0.1 μCi of [γ-^{32}P]NTP, and 0.2 mM unlabeled NTP. For nucleoside triphosphatase (NTPase) stimulation experiments 20 nM single-stranded DNA (ssDNA) (M13 mp18) or 20 nM double-stranded DNA (dsDNA) (pMS119EH) was added, and phospholipid micelles were prepared as described previously (36). The reaction was stopped by adding 2 μl of 0.5 M EDTA (pH 8.0). The reaction products were separated by thin-layer chromatography on 0.1-mm cellulose MN300 polyethyleneimine-impregnated sheets (POLYGRAM CEL 300 PEI; Macherey-Nagel) (48). Radioactive NTP and nucleoside diphosphate or P$_i$ were quantified by using storage phosphor technology (32) and the software ImageQuant 5.0 (Molecular Dynamics).

Gel filtration. Gen filtration with a Superdex 200 HR 10/30 column was performed as described previously (50) by using buffer A containing 5 mM MgCl$_2$ in the presence and in the absence of 0.2 mM ATP. The proteins applied to the column were 2 nmol of purified RP4 TrbEHNΔ2 and R388 TrwK, respectively.

DNA binding assays. For DNA binding assays 0.04, 0.4, and 4 nM purified RP4 TrbEHNΔ2 or R388 TrwK was mixed with 4 pM ssDNA (M13 mp18) or 3.2 pM dsDNA (pMS119EH) in the presence of 20 mM Tris-HCl (pH 7.6), 5 mM MgCl$_2$, and 0.05 mg of BSA per ml (final volume, 25 μl). The reaction mixtures were incubated for 30 min at 37°C, and then each mixture was mixed with 10 μl

of a solution containing 100 mM Tris-HCl (pH 7.6), 50% glycerol, and 0.1% bromophenol blue and electrophoresed on a 0.7% agarose gel.

Protein interaction analysis by surface plasmon resonance (SPR). Protein interaction was studied with the BIAcore system (Pharmacia Biosensor AB). Purified RP4 TrbEHNΔ2 protein (508 resonance units [RU]) was covalently coupled to flow cell 2 of Pioneer chip B1 with a BIAcore amine coupling kit. Flow cells 3 (loaded with 497 RU of BSA) and 4 (saturated with ethanolamine) were used as control cells. HBS-EP buffer (BIAcore) was used as the dilution and eluant buffer. Proteins RP4 TraG (50) and RP4 TrbB (36) were each injected at a concentration of 100 nM at a flow rate of 40 μl/min for 4 min. Dissociation was monitored for 5 min. Between injections, the flow cells were washed with 10 μl of a 200 mM Na$_2$CO$_3$ solution (pH 11.2).

Protein PRD1 P2 (22) (204 RU) was coupled to flow cell 2 of Pioneer chip CM5. Flow cells 3 (coupled with 512 RU of BSA) and 1 (saturated with ethanolamine) served as control cells. Proteins TrbEHNΔ2, TrbB, and PRD1 P2 were each injected at a concentration of 100 nM under the conditions described above.

RESULTS

Definition of four common motifs and one conserved domain in proteins belonging to the VirB4 family. The number of type IV secretion systems identified by sequence alignment has greatly increased in the last few years. To find out whether proteins belonging to the VirB4 family share characteristic features, we chose 18 of these proteins with the greatest similarity to RP4 TrbE and constructed a multiple-sequence alignment (Fig. 2). The overall similarity among these proteins is high and increases in the C-terminal half of the aligned sequences. The average length is about 800 to 830 amino acids. The smallest protein, TrbEb encoded by pNGR234a, consists of 662 residues, and the largest protein, *H. pylori* HP0544, is 983 amino acids long. TrbEa, encoded by pNGR234a directly upstream of *trbEb*, consists of 149 residues, and its sequence fits the N terminus of the aligned proteins well. Whether the

TABLE 4. Purification of RP4 TrbEHNΔ2 and R388 TrwK

Protein	Fraction	Purification step	Amt of protein (mg)	Yield (%)	Purity (%)[a]
TrbEHNΔ2	I	Crude cell extract	723	100	19
	II	Ni-NTA SF[b]	86	63	73
	III	Heparin Sepharose CL-6B	23	24	88
	IV	Phenyl Sepharose 6 Fast Flow	14	13	95
TrwK	I	Ammonium sulfate fraction	448	100	48
	II	Heparin Sepharose CL-6B	52	35	67
	III	Hydroxyapatite Bio-Gel HT	28	26	94
	IV	DEAE Sephacel	20	19	94

[a] Laser densitometric evaluation of Coomassie blue-stained SDS-polyacrylamide gels.
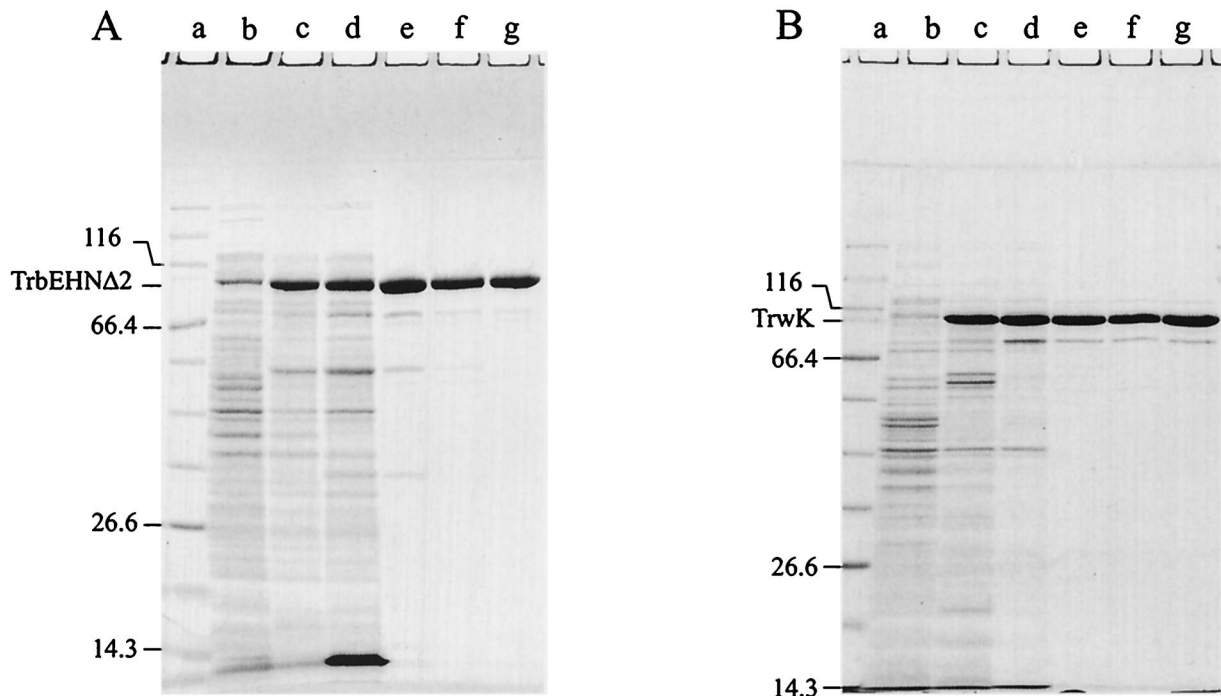[b] NTA, nitrilotriacetic acid.

FIG. 1. Purification of RP4 TrbEHNΔ2 (A) and R388 TrwK (B). Aliquots of extracts and pooled peak fractions (Table 4) were resolved with SDS–15% polyacrylamide gels and stained with Coomassie blue. Cells were lysed either by SDS or by Brij 58-lysozyme; the prominent band at an apparent mass of 14 kDa in panel A, lane d, is lysozyme. (A) Lane a, molecular mass standard; lanes b and c, SDS extracts of noninduced and IPTG-induced cells, respectively; lane d, fraction I (amount of total protein loaded onto the gel, 56.2 μg); lane e, fraction II (9.9 μg); lane f, fraction III (9.2 μg); lane g, fraction IV (10.1 μg). (B) Lane a, molecular mass standard; lanes b and c, SDS extracts of noninduced and IPTG-induced cells, respectively; lane d, fraction I (amount of total protein loaded onto the gel, 13.2 μg); lane e, fraction II (7.1 μg); lane f, fraction III (8.2 μg); lane g, fraction IV (7.4 μg).

gene products TrbEa and TrbEb exist and are essential remains to be determined.

All of the aligned sequences contain four motifs, which we designated motifs A, B, C, and D (Fig. 2, 3, and 4). Motif A represents Walker box A. It is the most prominent motif and is located near the middle of each of the aligned proteins. Motif B is Walker box B and consists of four hydrophobic residues followed by an aspartate (49). This motif is located approximately 180 residues after motif A and in most aligned proteins is represented by the sequence $h_4DE(A/F)W$, where h is a hydrophobic amino acid. For motif C we defined the consensus sequence $Dx_3(D/N)$ (where x represents any residue). Motif C is located between motifs A and B, and in RP4 TrbE it is represented by residues D642 to D646. In our alignment, R721 TraE is the only homologue containing an asparagine as the second conserved residue, and *H. pylori* HP0544 is the only protein with four residues between the conserved aspartate residues. For motif D we defined the consensus sequence $R(K/M)x_8(T/S)Q$. In most of the aligned sequences, motif D is represented by the sequence RKx_7ATQ (residues R717 to Q728 in RP4 TrbE).

In addition to these motifs, we designated a block of conserved residues domain I. Domain I comprises around 90 amino acids, including motifs B and D. In RP4 TrbE, the domain starts at residue F668 and ends at A757. Within domain I, a glycine, a threonine, and an isoleucine (G686, T748, and I750 in RP4 TrbE) are also conserved in all aligned pro-

teins. A conserved leucine and a conserved serine (L803 and S814 in RP4 TrbE) were found between domain I and the C terminus. A tyrosine (Y766 in RP4 TrbE) was found at similar positions in all proteins, and the W(L/I) residues (W837 and L838 in RP4 TrbE) near the C terminus were found in all proteins except *H. pylori* HP0544.

RP4 TrbE contains a predicted TMH at the N terminus (23). Interestingly, the only proteins in our alignment containing predicted N-terminal TMHs are the proteins encoded by RP4, R751, and pVT745, each of which has one helix, and the protein encoded by *H. pylori*, which has two consecutive TMHs.

The VirB4 protein family seems to consist of at least three subfamilies. These are the subfamily containing VirB4-like proteins with high similarity to Ti VirB4 proteins, the subfamily containing TrbE-like proteins with high similarity to RP4 TrbE, and the subfamily containing TraC-like proteins with high similarity to F TraC. In our alignment, VirB4-like proteins resemble the most comprehensive subfamily; TrbE-like proteins are represented by homologous proteins encoded by RP4, R751, pNGR234a, pRi1724, and pTiA6. Although TraC-like proteins encoded by plasmids F, R100-1, pNL1, and R27 have motifs A, B, and D, the similarity to VirB4 proteins is lower. Hence, this subfamily was not included in our alignment.

We found leucine zipper motifs in the family of VirB4 proteins. pTiC58 VirB4 and *Bartonella henselae* VirB4 contain
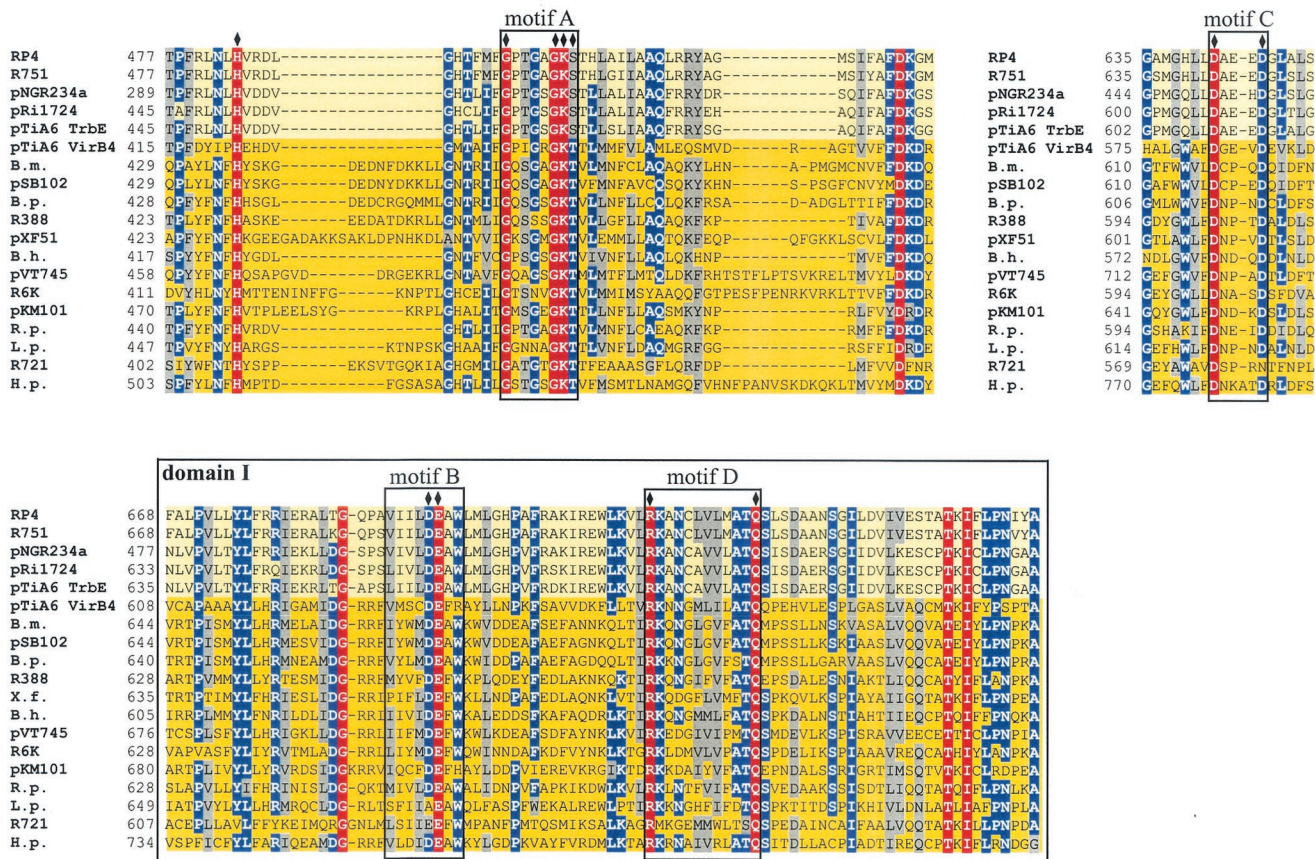
FIG. 2. Conserved motifs in proteins belonging to the VirB4 family. Walker boxes A (motif A) and B (motif B), motifs C and D, and domain I are conserved in a multiple-sequence alignment (red, conserved residues; blue, residues conserved in more than 70% of the sequences; gray, residues with similar side chains). The subfamily of TrbE-like proteins is indicated by a light yellow background, and the subfamily of VirB4-like proteins is indicated by a dark yellow background. Amino acids in RP4 TrbE which were subjected to site-directed mutagenesis are indicated by solid diamonds above the sequences. With the exception of TrbE and VirB4 encoded by pTiA6, only the name of the plasmid or bacterium encoding the protein homologous to VirB4 is given. The following VirB4 homologs were examined (the numbers in parentheses are accession numbers): RP4, TrbE (AAA26431); R751, TrbE (NP_044243); pNGR234a, TrbEb (AAB92432); pRi1724, TrbE (BAB16246); pTiA6 TrbE (AAB95097); pTiA6 VirB4 (AAF77164); *Brucella melitensis* VirB4 (B.m.) (AAL53269); pSB102, TraE (CAC79179); *Bordetella pertussis* PtlC (B.p.) (B47301); R388, TrwK (CAC78982); pXF51, XFa0007 (AAF85576); *Bartonella henselae* VirB4 (B.h.) (AAF00942); pVT745, MagB03 (AAG24434); R6K, Pilx4 (CAC20141); pKM101, TraB (I79267); *Rickettsia prowazekii* VirB4 (R.p.) (NP_220495); *Legionella pneumophila* LvhB4 (L.p.) (CAB60053); R721, TraE (NP_065362); and *H. pylori* HP0544 (H.p.) (NP_207340).

leucine zipper motifs at residues 302 to 323 and 303 to 324, respectively. Interestingly, pTiA6 VirB4, with 91.7% identity to pTiC58 VirB4, has the sequence $Lx_6Lx_6Mx_6L$ at the corresponding position. Several members of the VirB4-like subfamily contain a zipper-like motif which might resemble a bacterial zipper (20); examples include R388 TrwK containing the sequence $Ix_6Lx_6Mx_6L$ at positions 309 to 330 and *H. pylori* HP0544 and CagE encoded by strains HP26695 and J99, respectively, both of which contain the motif $Lx_6Vx_6Lx_6L$ at positions 459 to 480. In addition, both HP0544 and CagE contain a leucine zipper motif at residues 722 to 743. Members of the subfamily of TrbE-like proteins, however, contain neither a leucine zipper nor a leucine zipper-like motif at the corresponding positions. It remains to be determined whether these motifs in the VirB4 protein family have a function.

The multiple-sequence alignment of the VirB4 protein family revealed that proteins belonging to this family are very similar in terms of their primary structures, which might indi-cate that they also have similar tertiary or even quaternary structures.

Two-plasmid systems containing a nonpolar *trbE* in-frame deletion allow study of RP4 TrbE mutants in vivo. RP4 TrbE is essential for the Pil, Dps, and Tra phenotypes. To study the role of conserved motifs A to D in TrbE and to determine the essential portions of TrbE, we used two-plasmid systems which allowed in vivo tests of the function of TrbE mutants in *E. coli* to be performed (Table 3). The first plasmid, either pMS123Δ*trbE* for studying Pil and Dps or pDB126Δ*trbE* for studying Tra, encoded all essential transfer components except *trbE*. The second plasmid was the complementing plasmid pCR21 carrying either wild-type or mutated *trbE* (Table 2). Negative control strains were transformed with the vector plasmid pMS119HE instead of pCR21. As expected, the in-frame deletion of *trbE* with four original codons left at each terminus led to the Pil⁻, Dps⁻, and Tra⁻ phenotypes (transfer frequencies, $<10^{-7}$) (Table 2). Each of these phenotypes could be
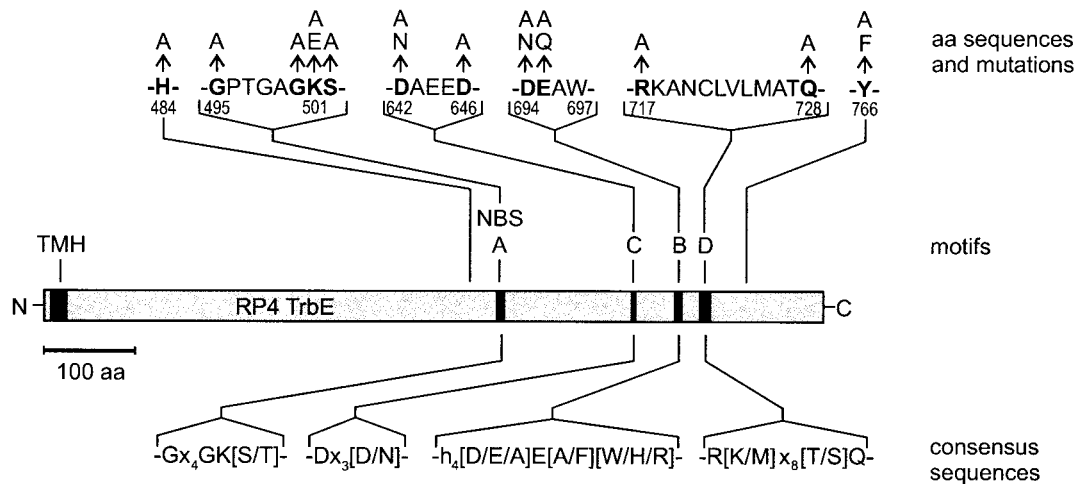
FIG. 3. Amino acid substitutions in RP4 TrbE and common motifs in the VirB4 protein family. Protein RP4 TrbE is represented by the gray bar. The predicted TMH and motifs A to D are represented by solid boxes. Each of the mutations influenced the Pil, Dps, and Tra phenotypes (Table 2). Proposed consensus sequences of the common motifs found in proteins belonging to the VirB4 family are shown below the bar. aa, amino acid; NBS, nucleotide binding site.

restored to wild-type levels with *trbE* in *trans*, indicating that the *trbE* in-frame deletion could be efficiently complemented and that expression of *trbE* downstream genes was not affected. We used these two-plasmid systems to genetically characterize RP4 TrbE (Table 2). To confirm that the mutant genes were expressed and that they were stable in the cells, we tested protein overproduction. With the exception of TrbEΔ1 (see below), all mutant proteins were overproduced after induction with 10 μM IPTG. The levels of expression of mutated genes

resulting in a negative or reduced phenotype were comparable to the level of expression in the wild type by Western blotting (data not shown). The cell extracts used were prepared from the strains used for transfer assays after 5 h of growth without IPTG induction.

Walker motifs A and B are essential for the in vivo function of RP4 TrbE. To determine the contributions of Walker motifs A and B and of residue H484 to the function(s) of TrbE, we exchanged conserved amino acids (Fig. 3) and tested the in

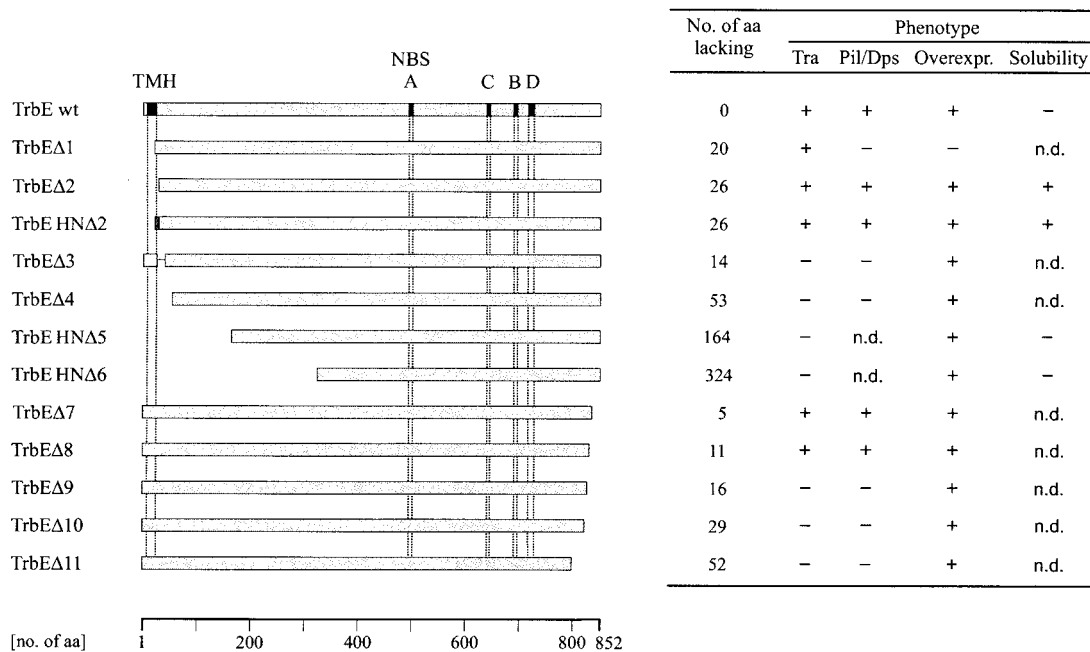|	No. of aa lacking	Phenotype			
		Tra	Pil/Dps	Overexpr.	Solubility
TrbE wt	0	+	+	+	−
TrbEΔ1	20	+	−	−	n.d.
TrbEΔ2	26	+	+	+	+
TrbE HNΔ2	26	+	+	+	+
TrbEΔ3	14	−	−	+	n.d.
TrbEΔ4	53	−	−	+	n.d.
TrbE HNΔ5	164	−	n.d.	+	−
TrbE HNΔ6	324	−	n.d.	+	−
TrbEΔ7	5	+	+	+	n.d.
TrbEΔ8	11	+	+	+	n.d.
TrbEΔ9	16	−	−	+	n.d.
TrbEΔ10	29	−	−	+	n.d.
TrbEΔ11	52	−	−	+	n.d.

FIG. 4. Phenotypes of RP4 TrbE deletion mutants. Wild-type TrbE and N- and C-terminal deletions are represented by gray bars. The predicted TMH and motifs A to D (Fig. 2) are indicated by solid boxes only in wild-type TrbE (TrbE wt). The His₆ tag at the N terminus of TrbEHNΔ2 is indicated by the dark gray box. The phenotypes of the mutants are indicated on the right. aa, amino acids; Overexpr., overexpression; n.d., not determined.

vivo activities of the mutants (Table 2). The H484A substitution reduced phage PRD1 adsorption but resulted in no further effects. With the exception of the G495A and K501A substitutions, all mutations within Walker motifs A and B led to a complete loss of the phenotypes tested. The partial activity of the K501A mutant was eliminated by the change from lysine to glutamate. With these experiments we showed that Walker motifs A and B are essential for pilus production, phage sensitivity, and DNA transfer. This finding strongly suggests that in vivo interaction of TrbE with nucleotides is required for TrbE function. Furthermore, our experiments indicate that the negative charges of amino acids D694 and E695 in Walker box B are likely to be essential for the protein's function(s).

Mutations in motifs C and D of RP4 TrbE influence phage sensitivity and DNA transfer. The functions of motifs C and D (Fig. 2) are not understood, and we found no previously published consensus sequence in the Swissprot database. To study the importance of these motifs for the function(s) of RP4 TrbE, we exchanged conserved amino acids and tested the in vivo effects of these mutations (Table 2). In addition, we mutated the codon for amino acid Y766. This tyrosine occurs at similar positions in all of the aligned proteins. All of these mutations influenced at least one of the phenotypes analyzed. Amino acid D642 was shown to be essential for the Pil, Dps, and Tra phenotypes, and the negative charge of this residue is likely to be essential. The amino acid substitutions Q728A, Y766A, and Y766F reduced phage PRD1 adsorption, but PRD1 propagation remained unaffected. This might indicate either that these residues in TrbE are essential for correct assembly of the PRD1 receptor or that these amino acids directly interact with a phage component. However, the PRD1 P2 protein did not interact with TrbEHNΔ2 in vitro (see below). The findings indicate that motifs C and D and the conserved tyrosine Y766 are important for the function(s) of RP4 TrbE.

Predicted TMH at the N terminus of RP4 TrbE is dispensable for Pil, Dps, and Tra. For RP4 TrbE, a TMH comprising amino acids I7 to I24 is predicted. To find out whether this predicted TMH is essential for the function of TrbE and how many residues of the N terminus are dispensable, we constructed several N-terminal deletion mutants (Fig. 4 and Table 2). With respect to Pil, Dps, and Tra, only two mutants, TrbEΔ2 and its His6-tagged derivative TrbEHNΔ2, behaved like the wild-type protein. These mutants lacked amino acids I2 to V27. In TrbEΔ1, residues I2 to F21 were deleted. Although 100-fold reduced, the deletion derivative retained the transferability but lost phage sensitivity completely. Although this mutant could not be overexpressed, we detected the protein with a specific antiserum after IPTG induction (data not shown). Seemingly, very low levels of TrbEΔ1 are sufficient for conjugation but probably not for phage adsorption. Mutant TrbEΔ3, carrying the predicted TMH but lacking residues A26 to K39, and TrbEΔ4, lacking residues I2 to D54, were nonfunctional. Mutants TrbEHNΔ5 and TrbEHNΔ6, constructed on the basis of supposed degradation products detected during protein purification (see below), were transfer deficient. We showed that 26 amino acids at the N terminus of TrbE containing the predicted TMH are dispensable for the Pil, Dps, and Tra phenotypes in *E. coli*. Removal of more than 26 N-terminal residues resulted in an immediate loss of TrbE activity, indi-

TABLE 5. Properties of RP4 TrbE, RP4 TrbEHNΔ2, R388 TrwK, and pTiA6 VirB4

Protein	No. of residues	Calculated mass (kDa)	Net charge[a]	Isoelectric point (calculated)
RP4 TrbE	852	94.4	−9	6.5
RP4 TrbEHNΔ2	833	92.6	−11	6.6
R388 TrwK	823	93.6	−27	5.2
pTiA6 VirB4	789	87.4	2	7.9

[a] The amino acids taken into account were D, E, R, and K.

cating that functional and/or structural integrity of the protein is essential.

C terminus of RP4 TrbE is important for protein function. A multiple-sequence alignment revealed high levels of similarity in the C-terminal halves of VirB4 proteins (Fig. 2). To determine the importance of the C terminus for RP4 TrbE, we constructed a series of deletion mutants (Fig. 4 and Table 2). The consistent effects of these mutants were either activities as detected for the wild-type protein (TrbEΔ7 and -8) or deficiencies for all phenotypes analyzed (TrbEΔ9, -10, and -11). The conserved amino acids W837 and L838 might be crucial for function, as deletion of these residues (TrbEΔ9) inactivated the protein. The tryptophan residue was found in all aligned proteins except *H. pylori* HP0544. With respect to the number of deleted amino acids, the C terminus of TrbE seemed to be even more sensitive than the N terminus.

N-terminal deletion of *trbE* yields a soluble protein. Wild-type *trbE* was cloned in an overexpression vector which allowed high levels of protein production. The full-length TrbE protein turned out to be insoluble even in 8 M urea. To overcome this problem, we constructed the deletion derivative *trbE*HNΔ2, whose product carried an N-terminal His6 tag and was fully functional in vivo (Table 2). Overexpression was induced with 10 μM IPTG, which for some reason resulted in higher protein levels than 1 mM IPTG. This phenomenon was also observed with the wild-type *trbE* gene. After induction, the cells divided one to two times. One prominent additional band at an apparent mass of approximately 90 kDa was detected in a sodium dodecyl sulfate (SDS)-polyacrylamide gel (Fig. 1). The mass of this protein is in good agreement with the calculated mass of TrbEHNΔ2 (Table 5). The purification steps used are summarized in Table 4. Eluted fractions from the Ni-nitrilotriacetic acid SF column contained four prominent additional bands that supposedly resulted from specific proteolysis of TrbEHNΔ2 (see below). The N-terminal sequence (MH6MDAE) of the purified full-length protein was confirmed.

Purification of R388 TrwK. Induction of SCS1(pCR38) cells with 1 mM IPTG and growth for 5 h resulted in overproduction of a protein with an apparent mass of approximately 97 kDa, which is in good agreement with the calculated mass of TrwK (Table 5). The purification steps used are summarized in Table 4. We found a potential degradation product of TrwK with an apparent mass of approximately 80 kDa (see below), which we could not separate from the full-length protein. The N-terminal sequence (GAIESR) of the purified protein was confirmed and revealed that the formyl-methionine was missing.

Overexpressed RP4 TrbEHNΔ2 and R388 TrwK contained

defined degradation products. During purification of RP4 TrbEHNΔ2 and R388 TrwK, we detected perplexing impurities that coeluted mostly with the desired proteins. To identify these impurities, we determined their N-terminal sequences. In the case of TrbEHNΔ2, the two major impurities started with the sequences KFVELM and KKWRQK, correlating with amino acids K166 and K326 of wild-type TrbE, respectively. Obviously, the overproduced protein had been specifically degraded. The apparent masses of these degradation products as determined with an SDS-polyacrylamide gel were approximately 70 and 52 kDa, respectively, and the calculated masses of the proteins were 76.2 and 58.0 kDa, respectively. Mainly the larger degradation product was difficult to separate from the full-length TrbEHNΔ2. The best separation of this impurity was obtained with phenyl Sepharose. In addition, gel filtration with a Superdex 200 HR 10/30 column (Amersham) was used to remove this impurity (data not shown). To test whether these truncated derivatives of TrbEHNΔ2 are biologically functional, we constructed the corresponding deletion mutants TrbEHNΔ5 (starting with amino acid F167) and TrbEHNΔ6 (starting with amino acid K326), both of which carry an N-terminal His₆ tag. The apparent masses of both proteins coincided with the masses of degradation products as determined with an SDS-polyacrylamide gel, suggesting that the C termini of the degradation products were intact. Both of these deletion derivatives were transfer deficient and, like wild-type TrbE, insoluble in 8 M urea.

The impurity detected during purification of R388 TrwK started with the sequence RERETP, correlating with residue R141 of the full-length protein and indicating that specific degradation occurred. This product was also detected when protease inhibitors (Complete EDTA-free; Roche Diagnostics, Mannheim, Germany) were present during purification (data not shown). TrwK was unstable during purification. Edman sequencing of purified TrwK also revealed the faint background sequence KLLASE, correlating with residue K7 of TrwK and indicating that there was some degradation near the N terminus.

Interestingly, the cleavage sites of the larger product of RP4 TrbEHNΔ2 and the product of R388 TrwK localized to almost identical positions in our sequence alignment. This might indicate that the tertiary structures of these proteins are similar, with a possible cleavage site exposed. All of the degradation products detected were apparently cleaved between an arginine and a lysine or vice versa. Overproduction of TrbEHNΔ2 in BL21 Star(DE3)(pLysS), which lacks Lon and OmpT proteases, did not eliminate this specific degradation. Probably, these proteins had been specifically degraded during overproduction, because degradation of TrbEΔ2 was also observed in cells cracked with SDS after overproduction.

Molecular cloning and overexpression of pTiA6 *virB4*. The pTiA6 *virB4* structural gene was cloned directly from plasmid pTiA6. We could not detect VirB4 after induction with 1 mM IPTG using SDS-polyacrylamide gel electrophoresis and Coomassie staining when the gene was translationally controlled by its original Shine-Dalgarno sequence, suggesting that the original ribosome binding site is not suitable for *E. coli*. We overexpressed *virB4* in strains BL21 and SCS1 (data not shown) after the gene was placed under translational control of the T7 gene *10* ribosome binding site and after addition of a second
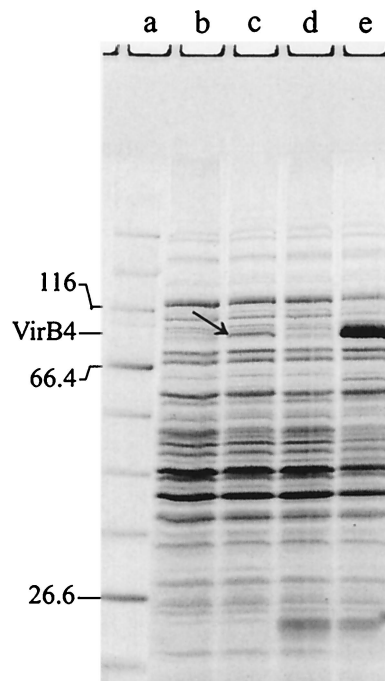

FIG. 5. Overproduction of pTiA6 VirB4 in *E. coli* strain BL21. Heterologous overexpression of *virB4* in *E. coli* is inhibited by different codon usage. The *virB4* gene contains 11 codons for arginine, nine codons for leucine, and two codons for proline, which are rare in *E. coli*. Plasmid pACYC-RIL encodes the tRNAs *argU* (AGA, AGG), *ileY* (AUA), and *leuW* (CUA). Freshly transformed strains BL21(pCR6) and BL21(pCR6, pACYC-RIL) were induced with 1 mM IPTG and grown for 5 h. Crude cell extracts of induced and noninduced cells were separated on an SDS–15% polyacrylamide gel and stained with Coomassie blue. Lane a, molecular mass standard; lane b, noninduced BL21(pCR6); lane c, induced BL21(pCR6); lane d, noninduced BL21(pCR6, pACYC-RIL); lane e, induced BL21(pCR6, pACYC-RIL). The arrow in lane c indicates the faint band of VirB4 resulting from induction in the absence of pACYC-RIL; the prominent band in lane e was shown to be VirB4.

plasmid encoding tRNAs that are rarely used by *E. coli* (Fig. 5). After induction we detected one prominent additional band at approximately 85 kDa, which is in good agreement with the calculated mass of pTiA6 VirB4 (Table 5). The N-terminal sequence (MLGASG) of the overproduced protein was confirmed. VirB4, which was overproduced at 37 or 25°C, was insoluble under nondenaturing conditions. After treatment with 8 M urea, we were unable to refold the polypeptide under several conditions.

Purified RP4 TrbEHNΔ2 and R388 TrwK did not hydrolyze ATP or GTP. Proteins belonging to the VirB4 family contain an ATP-GTP binding site and therefore are potential NTPases. To test whether purified TrbEHNΔ2 and TrwK hydrolyze ATP or GTP, we performed NTPase assays. Neither TrbEHNΔ2 nor TrwK hydrolyzed ATP or GTP under our standard conditions (pH 7.6, 5 mM MgCl₂). Varying the pH value (pH 6.0 and 9.0 with 5 mM MgCl₂), varying the MgCl₂ concentration (2 and 10 mM MgCl₂ at constant pH 7.6), and replacing 5 mM MgCl₂ with CaCl₂ as the bivalent cation at pH 7.6 did not result in ATP or GTP hydrolysis. Addition of
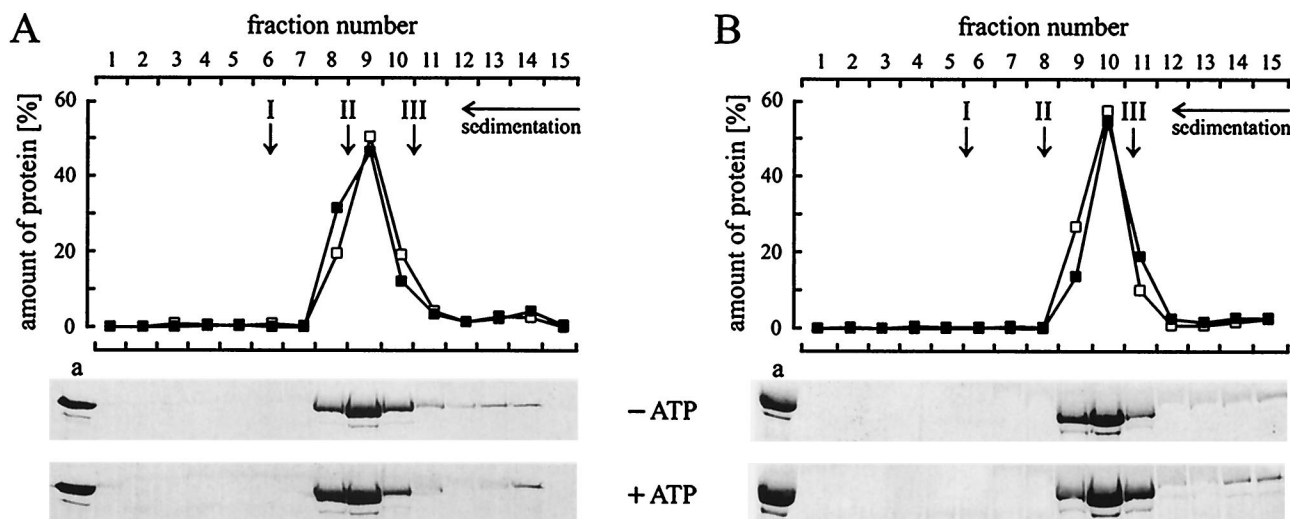
FIG. 6. Glycerol density gradient centrifugation of RP4 TrbEHNΔ2 (A) and R388 TrwK (B). Purified proteins TrbEHNΔ2 (fraction IV, 120 μl, 0.2 mg) (Table 4) and TrwK (fraction IV, 120 μl, 0.2 mg) (Table 4) were laid on a 3.8-ml, linear, 15 to 35% (wt/vol) glycerol gradient in buffer E. Protein samples were prepared in buffer E. For analysis of conformational changes, the samples were mixed with 1 mM ATP and 10 mM MgCl$_2$ and incubated for 10 min at 30°C prior to centrifugation. Centrifugation was carried out at 272,000 × g (r$_{max}$) for 18 h at 4°C. Fifteen fractions, each containing 15 drops of the gradient, were collected. Fifty microliters of each fraction and a 10-μl aliquot (lane a) of TrbEHNΔ2 or TrwK were separated on SDS–15% polyacrylamide gels. The gels were stained with Coomassie blue and scanned with a Personal densitometer (Molecular Dynamics). The amount of protein in each lane was quantified by using the software ImageQuant 5.0 (Molecular Dynamics). The relative amount of protein in each fraction is shown in the graphs (■, ATP and MgCl$_2$ added; □, ATP and MgCl$_2$ omitted). The arrows indicate the peak positions of the reference proteins (arrow I, catalase [240 kDa, $s_{20,w}$ = 11.3]; arrow II, aldolase [158 kDa, $s_{20,w}$ = 7.8]; arrow III, BSA [66 kDa, $s_{20,w}$ = 4.4]).

ssDNA or dsDNA did not induce ATP or GTP hydrolysis either.

The essential transfer components of RP4 contain the potential NTPases TrbE and TraG (50) and the weak ATPase TrbB (35, 36). To test whether these proteins can stimulate the ATPase activity of one another, we added TraG or TrbB or both of these proteins to TrbEHNΔ2 and carried out ATPase assays. We detected no increased nucleotide hydrolysis compared to that in control reaction mixtures containing only TraG or TrbB or both of these proteins. This finding indicates that neither of these proteins stimulates the ATPase activity of the other proteins used. Addition of ssDNA and dsDNA to a mixture containing TrbEHNΔ2, TraG, and TrbB did not stimulate ATPase activity either. Furthermore, we mixed these three proteins with ssDNA or dsDNA and then added micelles of phospatidylglycerol, phosphatidylethanolamine, or cardiolipin. We detected no increase in ATPase activity compared to that in a control reaction mixture containing only TrbB, indicating that the DNA and the phospholipids used are not sufficient to stimulate ATPase activity.

We suggest that RP4 TrbEHNΔ2 and R388 TrwK are not ATP-hydrolyzing proteins in vitro. However, we cannot exclude the possibility that additional cofactors are required for in vitro NTPase activity.

Purified RP4 TrbEHNΔ2 and R388 TrwK are monomeric proteins in solution. It has been suggested that pTiA6 VirB4 forms homodimers or homooligomers in vivo (15). To find out whether purified RP4 TrbEHNΔ2 and R388 TrwK are monomeric or oligomeric proteins in vitro, we used glycerol density gradient centrifugation and gel filtration. During glycerol density gradient centrifugation, TrbEHNΔ2 and TrwK sedimented as monomeric proteins, and addition of ATP together with

MgCl$_2$ as a bivalent cation had no effect (Fig. 6). The sedimentation coefficients ($s_{20,w}$) were determined to be 7.2 for TrbEHNΔ2 and 5.3 for TrwK. During gel filtration, TrbEHNΔ2 and TrwK eluted at apparent masses of 135 and 115 kDa, respectively. Addition of ATP to the buffer did not influence the elution profile, indicating that ATP does not greatly change the conformations and monomeric states of the proteins. The Stoke's radii of the proteins were determined to be 4.6 nm for TrbEHNΔ2 and 4.2 nm for TrwK. The frictional ratios (f/f_0) were calculated (53) to be 1.5 and 1.4 for TrbEHNΔ2 and TrwK, respectively. Hence, in vitro both proteins seem to be ellipsoids. Furthermore, no TrbEHNΔ2 self-interaction was detected by SPR (data not shown). Taken together, these results indicate that purified TrbEHNΔ2 and TrwK are monomeric and ellipsoidal proteins in solution.

RP4 TrbEHNΔ2 and R388 TrwK do not bind ssDNA and dsDNA. Both TrbEHNΔ2 and TrwK are proteins that are involved in the export of DNA. To determine whether TrbEHNΔ2 and TrwK interact with DNA, we carried out DNA binding assays. TrbEHNΔ2 did not retain ssDNA. A 1,000-fold excess of TrbEHNΔ2 weakly retained dsDNA. Such effects were also observed when BSA was used; therefore, this finding is considered a reflection of a nonphysiological interaction. TrwK retained neither ssDNA nor dsDNA. These results indicate that RP4 TrbEHNΔ2 and R388 TrwK have no DNA binding ability in vitro.

RP4 TrbEHNΔ2 does not interact with RP4 TraC, TraG, and TrbB and PRD1 P2. TrbE supposedly fulfills its function in close proximity to other plasmid-encoded proteins. To test possible protein-protein interactions in vitro, we used SPR. We found that TrbEHNΔ2 did not interact with TraC, a plasmid-encoded primase transferred with the DNA (44), did not in-

teract with TraG (50), and did not interact with the hexameric ATPase TrbB (35, 36).

The first step in phage PRD1 infection is mediated by the monomeric receptor binding protein P2 (22, 54). The composition of the receptor, however, is not known. Using SPR, we found that immobilized TrbEHNΔ2 did not interact with P2 and that immobilized PRD1 P2 protein did not interact with the Mpf components TrbB and TrbEHNΔ2 in vitro.

DISCUSSION

This study showed that the similarity among members of the VirB4 protein family is striking. We found four conserved motifs and one conserved domain (Fig. 2), and we showed for RP4 TrbE that the motifs are essential and/or important for the unknown function(s) of this transfer component. Analysis of N- and C-terminal deletion mutants revealed that both termini are important for the function(s) and/or the structure of TrbE. Our biochemical analysis of RP4 TrbEHNΔ2 and R388 TrwK revealed that these proteins do not hydrolyze ATP or GTP and that they are monomers in solution that do not bind ssDNA and dsDNA.

Components of type IV secretion systems which have identical functions are expected to have corresponding biochemical properties. This anticipation held true for VirB11-like proteins (35, 36, 63) and TraG-like proteins (50). However, the finding that the purified forms of RP4 TrbEHNΔ2 and R388 TrwK did not hydrolyze ATP is in contrast to the reported weak ATPase activity of pTiC58 VirB4 (52). Thus, we cannot exclude the possibility that VirB4 proteins have different biochemical properties according to the specific tasks of the corresponding export systems.

Interestingly, no ATPase activity could be found for several potential NTPases of conjugative plasmids and type IV secretion systems. For example, the TraG-like proteins RP4 TraG, R388 TrwB, *H. pylori* HP0524, and F TraD (50) do not hydrolyze nucleotides in vitro, but binding of nucleotides was demonstrated for RP4 TraG (E. Lanka and G. Schröder, unpublished data) and R388 TrwB (41). In addition, no ATPase activity could be detected for the potential NTPase RP4 TraL (E. Lanka, unpublished data), a soluble protein of unknown function necessary for efficient DNA transfer (39). Apparently, these potential NTPases, including members of the VirB4 protein family, for some reason do not possess NTPase activity in vitro. Possibly, the presence of additional plasmid-encoded and/or host factors is required. The VirB11-like proteins RP4 TrbB, R388 TrwD (45), and *H. pylori* HP0525 (35, 36) are the only proteins belonging to a defined family of potential NT-Pases for which a nucleotide-hydrolyzing activity was coincidentally shown.

To our knowledge, pTiA6 VirB4 is the only protein belonging to the VirB4 family that has been subjected to experimental determination of its topology. Although secondary-structure predictions revealed no TMHs for VirB4, Dang and Christie (14) suggested that VirB4 is an inner membrane protein with four membrane-spanning α-helical segments, resulting in three cytoplasmic and two periplasmic domains. The charged amino acids within these helices do not conflict but could be required for specific domain interactions. With reference to our multiple-sequence alignment, these four helices in pTiA6 VirB4

correlate with conserved regions in the VirB4 protein family. In VirB4, helices 1 and 2 (analogous to RP4 TrbE residues L46 to A68 and F140 to Q164, respectively) contain several amino acids that are conserved in more than 70% of the aligned proteins (data not shown). Interestingly, the cleavage sites for the supposed specific degradation of RP4 TrbEHNΔ2 and R388 TrwK are located at the C-terminal end of helix 2. As determined by topology studies of VirB4 (14), Walker box A is located in the cytoplasm at the N terminus of helix 3 (analogous to RP4 TrbE residues S502 to G526). With regard to the primary structure, helix 4 (RP4 TrbE residues F668 to L684) starts exactly at the beginning of domain I (Fig. 2) and ends two amino acids before the conserved glycine (RP4 TrbE residue G686). In this model, Walker motifs A and B are located in the cytoplasm and could be in the immediate vicinity for concerted interactions with nucleotides. The four proposed TMHs in VirB4 correlate with conserved regions in the VirB4 protein family (Fig. 2). Hence, our findings support this topology model and indicate that the topology for proteins belonging to the VirB4 family is similar.

How does the exchange of homologous proteins affect conjugation? The proteins R388 TrwK, pTiA6 VirB4, and R1-16 TraC and the two homologues VirB4 and TrwK encoded by the mammalian pathogen *Bartonella tribocorum* (5) could not complement the RP4 Δ*trbE* deletion mutant with respect to DNA transfer ability (data not shown). Similar studies with TraG-like proteins (11, 28) and RP4 TrbC (17) revealed either that the systems are nonfunctional or that the transfer efficiency was reduced by several orders of magnitude. Hence, proteins of conjugation and type IV secretion systems are highly specialized in their original system. The proteins show system specificity and can be interchanged only with loss of the conjugation or secretion activity.

Could proteins of the VirB4 family be the Achilles' heel of conjugation and type IV secretion systems? Depending on the situation, such export systems could also waste energy or adversely affect the cell surface (for instance, by making the host sensitive to lytic phages). Proteins belonging to the VirB4 family were found to be the largest components of Mpf and type IV secretion systems, and they were shown to be essential for each of these systems studied in detail. As a consequence, a large and essential gene coding for a core component of a multiprotein complex would be the ideal candidate for a host to dispose of a detrimental system. Our point mutations and deletions in *trbE* showed how sensitively the RP4 transfer system responds to even slight interference. In addition, none of the homologous VirB4 proteins tested could replace TrbE in the RP4 system. In RP4, spontaneous mutations leading to phage PRD1 resistance were almost exclusively mapped in *trbC*, *-E*, and *-L*, either indicating hot spots within these genes or pointing out the importance of the corresponding proteins for PRD1 receptor formation (24). The plant pathogen *Xylella fastidiosa*, for example, carries three genes for VirB4 proteins, pXF51 *xfa0007* (Fig. 2), the chromosomal gene *xf2053*, and pXF51 *xfa0044*. The latter two genes were seemingly knocked out by mutations that resulted in an early stop codon and a frameshift, respectively. Presumably, three copies of one homologous protein were detrimental to the host.

The increasing availability of sequence information should allow detection of more type IV secretion systems and enlarge-

ment of the VirB4 protein family. For instance, sequencing of *A. tumefaciens* C58 revealed that this plant pathogen contains two chromosomes and two plasmids and carries in addition to VirB and Trb a third type IV secretion system, namely, AvhB (21, 61). The human pathogen *H. pylori* strain HP26695 contains four genes encoding VirB4 proteins HP0544, ComB4 (31), HP0441, and HP0459. Although the fascinating insights into these genomes raise many questions regarding the biology of these pathogens, we point out that for many members of the VirB4 family the existence of the proteins and the functional context remain to be determined.

ACKNOWLEDGMENTS

ADDENDUM IN PROOF

We examined the negative dominance of the amino acid substitutions TrbEG500A, K501A, K501E, S502A, D642A, D642N, D646A, D694A, D694N, E695A, E695Q, R717A, Q728A, Y766A, and Y766F and the N-terminal deletion mutation TrbEΔ1 in the presence of wt TrbE. The transfer frequencies of strain HB101 carrying pDB126 (wt *trbE*) and pCR21 (mutant *trbE*) were determined. All mutants except D646A, Y766A, and Y766F exhibited a negative dominant phenotype compared to cells coexpressing wt *trbE* from pDB126 and pCR21. This result indicates that mutant *trbE* genes are expressed and that the gene products supposedly interfere with the function of the assembled RP4 Mpf complex.

REFERENCES

1. **Altschul, S. F., T. L. Madden, A. A. Schaffer, J. Zhang, Z. Zhang, W. Miller, and D. J. Lipman.** 1997. Gapped BLAST and PSI-BLAST: a new generation of protein database search programs. Nucleic Acids Res. **25:**3389–3402.
2. **Balzer, D., W. Pansegrau, and E. Lanka.** 1994. Essential motifs of relaxase (TraI) and TraG proteins involved in conjugative transfer of plasmid RP4. J. Bacteriol. **176:**4285–4295.
3. **Balzer, D., G. Ziegelin, W. Pansegrau, V. Kruft, and E. Lanka.** 1992. KorB protein of promiscuous plasmid RP4 recognizes inverted sequence repetitions in regions essential for conjugative plasmid transfer. Nucleic Acids Res. **20:**1851–1858.
4. **Bamford, D. H., L. Rouhiainen, K. Takkinen, and H. Soderlund.** 1981. Comparison of the lipid-containing bacteriophages PRD1, PR3, PR4, PR5 and L17. J. Gen. Virol. **57:**365–373.
5. **Baron, C., D. O'Callaghan, and E. Lanka.** 2002. Bacterial secrets of secretion: EuroConference on the Biology of Type IV Secretion Processes. Mol. Microbiol. **43:**1359–1365.
6. **Berger, B. R., and P. J. Christie.** 1993. The *Agrobacterium tumefaciens virB4* gene product is an essential virulence protein requiring an intact nucleoside triphosphate-binding domain. J. Bacteriol. **175:**1723–1734.
7. **Bolland, S., M. Llosa, P. Avila, and F. de la Cruz.** 1990. General organization of the conjugal transfer genes of the IncW plasmid R388 and interactions between R388 and IncN and IncP plasmids. J. Bacteriol. **172:**5795–5802.
8. **Boyer, H. W., and D. Roulland-Dussoix.** 1969. A complementation analysis of the restriction and modification of DNA in *Escherichia coli.* J. Mol. Biol. **41:**459–472.
9. **Bradley, D. E.** 1980. Determination of pili by conjugative bacterial drug resistance plasmids of incompatibility groups B, C, H, J, K, M, V, and X. J. Bacteriol. **141:**828–837.
10. **Burns, D. L.** 1999. Biochemistry of type IV secretion. Curr. Opin. Microbiol. **2:**25–29.
11. **Cabezón, E., J. I. Sastre, and F. de la Cruz.** 1997. Genetic evidence of a coupling role for the TraG protein family in bacterial conjugation. Mol. Gen. Genet. **254:**400–406.
12. **Christie, P. J.** 2001. Type IV secretion: intercellular transfer of macromolecules by systems ancestrally related to conjugation machines. Mol. Microbiol. **40:**294–305.
13. **Christie, P. J., and J. P. Vogel.** 2000. Bacterial type IV secretion: conjugation systems adapted to deliver effector molecules to host cells. Trends Microbiol. **8:**354–360.
14. **Dang, T. A., and P. J. Christie.** 1997. The VirB4 ATPase of *Agrobacterium tumefaciens* is a cytoplasmic membrane protein exposed at the periplasmic surface. J. Bacteriol. **179:**453–462.
15. **Dang, T. A., X. R. Zhou, B. Graf, and P. J. Christie.** 1999. Dimerization of the *Agrobacterium tumefaciens* VirB4 ATPase and the effect of ATP-binding cassette mutations on the assembly and function of the T-DNA transporter. Mol. Microbiol. **32:**1239–1253.
16. **di Jeso, F.** 1968. Ammonium sulfate concentration conversion nomograph for 0 degrees. J. Biol. Chem. **243:**2022–2023.
17. **Eisenbrandt, R.** 1999. Macromolecular export systems, identification of conjugative pilins and their modification. Ph.D. thesis. Technische Universität Berlin, Berlin, Germany.
18. **Eisenbrandt, R., M. Kalkum, E. M. Lai, R. Lurz, C. I. Kado, and E. Lanka.** 1999. Conjugative pili of IncP plasmids and the Ti plasmid T pilus are composed of cyclic subunits. J. Biol. Chem. **274:**22548–22555.
19. **Fullner, K. J., K. M. Stephens, and E. W. Nester.** 1994. An essential virulence protein of *Agrobacterium tumefaciens,* VirB4, requires an intact mononucleotide binding domain to function in transfer of T-DNA. Mol. Gen. Genet. **245:**704–715.
20. **Giraldo, R., C. Nieto, M. E. Fernández-Tresguerres, and R. Díaz.** 1989. Bacterial zipper. Nature **342:**866.
21. **Goodner, B., G. Hinkle, S. Gattung, N. Miller, M. Blanchard, B. Qurollo, B. S. Goldman, Y. Cao, M. Askenazi, C. Halling, L. Mullin, K. Houmiel, J. Gordon, M. Vaudin, O. Iartchouk, A. Epp, F. Liu, C. Wollam, M. Allinger, D. Doughty, C. Scott, C. Lappas, B. Markelz, C. Flanagan, C. Crowell, J. Gurson, C. Lomo, C. Sear, G. Strub, C. Cielo, and S. Slater.** 2001. Genome sequence of the plant pathogen and biotechnology agent *Agrobacterium tumefaciens* C58. Science **294:**2323–2328.
22. **Grahn, A. M., J. Caldentey, J. K. Bamford, and D. H. Bamford.** 1999. Stable packaging of phage PRD1 DNA requires adsorption protein P2, which binds to the IncP plasmid-encoded conjugative transfer complex. J. Bacteriol. **181:**6689–6696.
23. **Grahn, A. M., J. Haase, D. H. Bamford, and E. Lanka.** 2000. Components of the RP4 conjugative transfer apparatus form an envelope structure bridging inner and outer membranes of donor cells: implications for related macromolecule transport systems. J. Bacteriol. **182:**1564–1574.
24. **Grahn, A. M., J. Haase, E. Lanka, and D. H. Bamford.** 1997. Assembly of a functional phage PRD1 receptor depends on 11 genes of the IncP plasmid mating pair formation complex. J. Bacteriol. **179:**4733–4740.
25. **Haase, J., M. Kalkum, and E. Lanka.** 1996. TrbK, a small cytoplasmic membrane lipoprotein, functions in entry exclusion of the IncPα plasmid RP4. J. Bacteriol. **178:**6720–6729.
26. **Haase, J., and E. Lanka.** 1997. A specific protease encoded by the conjugative DNA transfer systems of IncP and Ti plasmids is essential for pilus synthesis. J. Bacteriol. **179:**5728–5735.
27. **Haase, J., R. Lurz, A. M. Grahn, D. H. Bamford, and E. Lanka.** 1995. Bacterial conjugation mediated by plasmid RP4: RSF1010 mobilization, donor-specific phage propagation, and pilus production require the same Tra2 core components of a proposed DNA transport complex. J. Bacteriol. **177:**4779–4791.
28. **Hamilton, C. M., H. Lee, P. L. Li, D. M. Cook, K. R. Piper, S. B. von Bodman, E. Lanka, W. Ream, and S. K. Farrand.** 2000. TraG from RP4 and TraG and VirD4 from Ti plasmids confer relaxosome specificity to the conjugal transfer system of pTiC58. J. Bacteriol. **182:**1541–1548.
29. **Hanahan, D.** 1983. Studies on transformation of *Escherichia coli* with plasmids. J. Mol. Biol. **166:**557–580.
30. **Heinemann, J. A., and G. F. Sprague, Jr.** 1989. Bacterial conjugative plasmids mobilize DNA transfer between bacteria and yeast. Nature **340:**205–209.
31. **Hofreuter, D., S. Odenbreit, and R. Haas.** 2001. Natural transformation competence in *Helicobacter pylori* is mediated by the basic components of a type IV secretion system. Mol. Microbiol. **41:**379–391.
32. **Johnston, R. F., S. C. Pickett, and D. L. Barker.** 1990. Autoradiography using storage phosphor technology. Electrophoresis **11:**355–360.
33. **Kalkum, M., R. Eisenbrandt, R. Lurz, and E. Lanka.** 2002. Tying rings for sex. Trends Microbiol. **10:**382–387.
34. **Kotilainen, M. M., A. M. Grahn, J. K. Bamford, and D. H. Bamford.** 1993. Binding of an *Escherichia coli* double-stranded DNA virus PRD1 to a receptor coded by an IncP-type plasmid. J. Bacteriol. **175:**3089–3095.
35. **Krause, S., M. Bárcena, W. Pansegrau, R. Lurz, J. M. Carazo, and E. Lanka.** 2000. Sequence-related protein export NTPases encoded by the conjugative

transfer region of RP4 and by the *cag* pathogenicity island of *Helicobacter pylori* share similar hexameric ring structures. Proc. Natl. Acad. Sci. USA **97:**3067–3072.

36. **Krause, S., W. Pansegrau, R. Lurz, F. de la Cruz, and E. Lanka.** 2000. Enzymology of type IV macromolecule secretion systems: the conjugative transfer regions of plasmids RP4 and R388 and the *cag* pathogenicity island of *Helicobacter pylori* encode structurally and functionally related nucleoside triphosphate hydrolases. J. Bacteriol. **182:**2761–2770.

37. **Lessl, M., D. Balzer, R. Lurz, V. L. Waters, D. G. Guiney, and E. Lanka.** 1992. Dissection of IncP conjugative plasmid transfer: definition of the transfer region Tra2 by mobilization of the Tra1 region in *trans*. J. Bacteriol. **174:**2493–2500.

38. **Lessl, M., D. Balzer, W. Pansegrau, and E. Lanka.** 1992. Sequence similarities between the RP4 Tra2 and the Ti VirB region strongly support the conjugation model for T-DNA transfer. J. Biol. Chem. **267:**20471–20480.

39. **Lessl, M., D. Balzer, K. Weyrauch, and E. Lanka.** 1993. The mating pair formation system of plasmid RP4 defined by RSF1010 mobilization and donor-specific phage propagation. J. Bacteriol. **175:**6415–6425.

40. **Miller, J. H.** 1972. Experiments in molecular genetics, p. 431–433. Cold Spring Harbor Laboratory Press, Cold Spring Harbor, N.Y.

41. **Moncalián, G., E. Cabezón, I. Alkorta, M. Valle, F. Moro, J. M. Valpuesta, F. M. Goñi, and F. de la Cruz.** 1999. Characterization of ATP and DNA binding activities of TrwB, the coupling protein essential in plasmid R388 conjugation. J. Biol. Chem. **274:**36117–36124.

42. **Olsen, R. H., and D. D. Thomas.** 1973. Characteristics and purification of PRR1, an RNA phage specific for the broad host range *Pseudomonas* R1822 drug resistance plasmid. J. Virol. **12:**1560–1567.

43. **Pansegrau, W., and E. Lanka.** 1996. Enzymology of DNA transfer by conjugative mechanisms. Prog. Nucleic Acid Res. Mol. Biol. **54:**197–251.

44. **Pansegrau, W., E. Lanka, P. T. Barth, D. H. Figurski, D. G. Guiney, D. Haas, D. R. Helinski, H. Schwab, V. A. Stanisich, and C. M. Thomas.** 1994. Complete nucleotide sequence of Birmingham IncPα plasmids. Compilation and comparative analysis. J. Mol. Biol. **239:**623–663.

45. **Rivas, S., S. Bolland, E. Cabezón, F. M. Goni, and F. de la Cruz.** 1997. TrwD, a protein encoded by the IncW plasmid R388, displays an ATP hydrolase activity essential for bacterial conjugation. J. Biol. Chem. **272:**25583–25590.

46. **Sambrook, J., E. F. Fritsch, and T. Maniatis.** 1989. Molecular cloning: a laboratory manual, 2nd ed. Cold Spring Harbor Laboratory, Cold Spring Harbor, N.Y.

47. **Sano, T., and C. R. Cantor.** 1990. Expression of a cloned streptavidin gene in *Escherichia coli*. Proc. Natl. Acad. Sci. USA **87:**142–146.

48. **Scherzinger, E., G. Ziegelin, M. Bárcena, J. M. Carazo, R. Lurz, and E. Lanka.** 1997. The RepA protein of plasmid RSF1010 is a replicative DNA helicase. J. Biol. Chem. **272:**30228–30236.

49. **Schneider, E., and S. Hunke.** 1998. ATP-binding-cassette (ABC) transport systems: functional and structural aspects of the ATP-hydrolyzing subunits/domains. FEMS Microbiol. Rev. **22:**1–20.

50. **Schröder, G., S. Krause, E. L. Zechner, B. Traxler, H. J. Yeo, R. Lurz, G. Waksman, and E. Lanka.** 2002. TraG-like proteins of DNA transfer systems and of the *Helicobacter pylori* type IV secretion system: inner membrane gate for exported substrates? J. Bacteriol. **184:**2767–2779.

51. **Shirasu, K., and C. I. Kado.** 1993. The *virB* operon of the *Agrobacterium tumefaciens* virulence regulon has sequence similarities to B, C and D open reading frames downstream of the pertussis toxin-operon and to the DNA transfer-operons of broad-host-range conjugative plasmids. Nucleic Acids Res. **21:**353–354.

52. **Shirasu, K., Z. Koukolíková-Nicola, B. Hohn, and C. I. Kado.** 1994. An inner-membrane-associated virulence protein essential for T-DNA transfer from *Agrobacterium tumefaciens* to plants exhibits ATPase activity and similarities to conjugative transfer genes. Mol. Microbiol. **11:**581–588.

53. **Siegel, L. M., and K. J. Monty.** 1966. Determination of molecular weights and frictional ratios of proteins in impure systems by use of gel filtration and density gradient centrifugation. Application to crude preparations of sulfite and hydroxylamine reductases. Biochim. Biophys. Acta **112:**346–362.

54. **Sokolova, A., M. Malfois, J. Caldentey, D. I. Svergun, M. H. Koch, D. H. Bamford, and R. Tuma.** 2001. Solution structure of bacteriophage PRD1 vertex complex. J. Biol. Chem. **276:**46187–46195.

55. **Stanisich, V. A.** 1974. The properties and host range of male-specific bacteriophages of *Pseudomonas aeruginosa*. J. Gen. Microbiol. **84:**332–342.

56. **Strack, B., M. Lessl, R. Calendar, and E. Lanka.** 1992. A common sequence motif, -E-G-Y-A-T-A-, identified within the primase domains of plasmid-encoded I- and P-type DNA primases and the α protein of the *Escherichia coli* satellite phage P4. J. Biol. Chem. **267:**13062–13072.

57. **Thompson, J. D., D. G. Higgins, and T. J. Gibson.** 1994. CLUSTAL W: improving the sensitivity of progressive multiple sequence alignment through sequence weighting, position-specific gap penalties and weight matrix choice. Nucleic Acids Res. **22:**4673–4680.

58. **Walker, J. E., M. Saraste, M. J. Runswick, and N. J. Gay.** 1982. Distantly related sequences in the α- and β-subunits of ATP synthase, myosin, kinases and other ATP-requiring enzymes and a common nucleotide binding fold. EMBO J. **1:**945–951.

59. **Waters, V. L.** 2001. Conjugation between bacterial and mammalian cells. Nat. Genet. **29:**375–376.

60. **Weiner, M. P., G. L. Costa, W. Schoettlin, J. Cline, E. Mathur, and J. C. Bauer.** 1994. Site-directed mutagenesis of double-stranded DNA by the polymerase chain reaction. Gene **151:**119–123.

61. **Wood, D. W., J. C. Setubal, R. Kaul, D. E. Monks, J. P. Kitajima, V. K. Okura, Y. Zhou, L. Chen, G. E. Wood, N. F. Almeida, Jr., L. Woo, Y. Chen, I. T. Paulsen, J. A. Eisen, P. D. Karp, D. Bovee, Sr., P. Chapman, J. Clendenning, G. Deatherage, W. Gillet, C. Grant, T. Kutyavin, R. Levy, M. J. Li, E. McClelland, A. Palmieri, C. Raymond, G. Rouse, C. Saenphimma-chak, Z. Wu, P. Romero, D. Gordon, S. Zhang, H. Yoo, Y. Tao, P. Biddle, M. Jung, W. Krespan, M. Perry, B. Gordon-Kamm, L. Liao, S. Kim, C. Hendrick, Z. Y. Zhao, M. Dolan, F. Chumley, S. V. Tingey, J. F. Tomb, M. P. Gordon, M. V. Olson, and E. W. Nester.** 2001. The genome of the natural genetic engineer *Agrobacterium tumefaciens* C58. Science **294:**2317–2323.

62. **Yanisch-Perron, C., J. Vieira, and J. Messing.** 1985. Improved M13 phage cloning vectors and host strains: nucleotide sequences of the M13mp18 and pUC19 vectors. Gene **33:**103–119.

63. **Yeo, H. J., S. N. Savvides, A. B. Herr, E. Lanka, and G. Waksman.** 2000. Crystal structure of the hexameric traffic ATPase of the *Helicobacter pylori* type IV secretion system. Mol. Cell **6:**1461–1472.